CRCLEME
Cooperative Research Centre for Landscape Environments and Mineral Exploration

action Salinity & Water AUSTRALIA

Government of South Australia

OPEN FILE REPORT SERIES

ANU THE AUSTRALIAN NATIONAL UNIVERSITY

CSIRO

THE VALIDATION OF RESOLVE HELICOPTER EM DATA: MINERALOGICAL AND PETROPHYSICAL RESULTS FROM FIELD INVESTIGATIONS IN THE RIVERLAND AREA, SOUTH AUSTRALIA

K.P Tan, T. Munday and F. Leaney

CRC LEME OPEN FILE REPORT 179

September 2004

THE VALIDATION OF RESOLVE HELICOPTER EM DATA: MINERALOGICAL AND PETROPHYSICAL RESULTS FROM FIELD INVESTIGATIONS IN THE RIVERLAND AREA, SOUTH AUSTRALIA

K.P Tan, T. Munday and F. Leaney

CRC LEME OPEN FILE REPORT 179

September 2004

Report prepared for the South Australia Salinity Mapping and Management Support Project.
This project is jointly funded by the South Australian and Commonwealth Governments under the National Action Plan for Salinity and Water Quality.

CRC LEME is an unincorporated joint venture between CSIRO-Exploration & Mining, and Land and Water, The Australian National University, Curtin University of Technology, University of Adelaide, Geoscience Australia, Primary Industries and Resources SA, NSW Department of Mineral Resources and Minerals Council of Australia.

Headquarters: CRC LEME c/o CSIRO Exploration and Mining, PO Box 1130, Bentley WA 6102, Australia

Copies of this Publication can be obtained from :
The publications Officer, CRCLEME, c/- CSIRO Exploration and Mining, PO Box 1130, Bentley WA 6120, Australia. Information on other publications in this series may be obtained from the above, or from http://crcleme.org.au
Cataloguing-in-Publication:
Name: Tan, K.P, Munday T.J. and Leaney, F.W.J., Title: The validation of RESOLVE Helicopter EM data: mineralogical and petrophysical results from field investigations in the Riverland Area, South Australia
ISBN 1 921039 17 5
1.Riverland, South Australia 2. AEM 3. Petrophysics
I. Name II. Title
CRCLEME Open File Report 178
ISSN 1329-4768

Address and Affiliation of Authors

KP Tan
Cooperative Research Centre for Landscape Environments and Mineral Exploration
Geoscience Australia
GPO Box 378,
Canberra, ACT 2601
Australia

Tim Munday
Cooperative Research Centre for Landscape Environments and Mineral Exploration
c/- CSIRO Exploration and Mining
26 Dick Perry Avenue,
Technology Park,
Kensington, Western Australia 6151
Australia.

Fred Leaney
CSIRO Land and Water
PMB 2
Glen Osmond
South Australia 5064
Australia

Table of Contents

List of Figures

List of Tables **Page**

ABSTRACT

As part of the South Australia Salinity Mapping and Management Support Project (SA-SMMSP), the Riverland project was set up to use airborne electromagnetic (AEM) data to map the near surface distribution of fine textured materials at an appropriate resolution to provide information for determining recharge rates to the saline groundwater which forms the basis for managing salt being discharged into the River Murray A frequency domain helicopter electromagnetic system (RESOLVE) was selected to delineate the near surface conductors, which are mainly associated with fine-textured materials such as the Pleistocene Blanchetown Clay unit.

The study had two specific objectives:

1. To define the principal factors driving variations in electrical conductivity in the sediments of the Riverland region.
2. To ascertain whether the conductive patterns shown in the high frequency apparent conductivity data (eg. 100,000 Hz and 25,000 Hz) and EM inversion products such as conductivity depth imaging (CDI's) and the "Clay Thickness Map" accurately reflect the distribution of clay materials.

These objectives were achieved through targeted drilling, geological logging, the geochemical, mineralogical and petrophysical analysis of bore cuttings and cores, and acquisition of borehole geophysical logs, including conductivity and natural gamma. From an analysis of the laboratory results, geophysical logs and cross referencing with the inverted EM data the following can be concluded.

1. In the Riverland survey area, variations in the observed apparent electrical conductivity (ECa) of near surface materials are primarily determined by the texture of sediments. A detailed analysis of texture and water content established that finer textured materials are generally characterized by higher water contents. Although chloride concentrations may vary, and remain high in sand-rich materials, the low water content associated with sand and the higher water content associated with clay-rich sediments resulted in a low ECa for the former and an elevated ECa for the latter.

2. Textural information and borehole conductivity logs obtained from the 14 selected boreholes, which target specific conductivity patterns shown on the high frequency (25,000 Hz) apparent conductivity image, suggest that the observed conductivity response is largely determined by the distribution of near surface clayey materials. A discrepancy arises in the vicinity of low lying areas where shallow and saline groundwater occurs, in which case, the conductivity signature is attributed to conductive saturated sand. A comparison between inversion procedures (apparent conductivity, CDI and a constrained 1D Layered Earth Inversion) in the vicinity of borehole RIV9HC and RIV9LC shows that the RESOLVE HEM system is capable of differentiating between conductive shallow clay and a saline, conductive groundwater (i.e. saturated sand). The best results from a clay mapping perspective, were obtained from the constrained inversion confirming the value of a full inversion in reducing ambiguities.

1. INTRODUCTION

The South Australian Riverland region, located between the border and Morgan, is known to contribute significantly to the salinisation of the River Murray, much of it attributed to increases in discharge from a saline groundwater system. The rise in groundwater is a direct consequence of increases in recharge from irrigation and clearing of native vegetation. Whilst improved irrigation practice and interception schemes have helped reduce the salt input into the river, pressure for further developments require additional strategies to minimize reliance on relatively high cost salt interception schemes and their "off-site" penalty. Low recharge agricultural practices and the considered development and management of irrigation are among the options, but both require an improved understanding of the soil and sediments found across the Riverland region. The texture of near-surface soils and sediments is known to influence recharge rates (Cook *et al.*, 2001, Leaney *et al.*, 2004), with lower rates observed over shallow clay-rich materials, including the Blanchetown Clay. However, information on the spatial distribution and variability (including thickness) of these materials is limited to scattered exploration boreholes or clustered irrigation bores, and limited outcrops.

Previous work around Borrika, to the south of the Riverland region, had established that near-surface clay-rich materials, where present, are characterized by elevated electrical conductivities relative to overlying and underlying sedimentary/regolith units. As a consequence, they could be mapped using helicopter airborne electromagnetic (HEM) system (Cook and Kilty 1992). Trial results with a similar HEM system in the Riverland itself (Munday *et al.*, 2003) confirmed these findings and suggested that both the thickness and distribution of these shallow clays, including the Blanchetown Clay unit, could be mapped at scales which would allow more reliable and detailed predictions of the effects of particular management options on recharge when used as an input into numerical recharge and groundwater models.

As part of the South Australia Salinity Mapping and Management Support Project (SA-SMMSP), a high resolution HEM survey was completed for part of the Riverland region in late 2002. In support of this survey we undertook to acquire ancillary ground data through drilling and field observations to help constrain our interpretation and analysis of the resulting data, and to provide us with some indication as to how reliable the system was as a mapping tool.

2. OBJECTIVES

The primary objective of this study was to validate causes for the observed conductivity structure in the RESOLVE HEM data and provide a basis for their interpretation. The intent was to further validate these data as an effective technology for mapping near surface, "clay" rich sedimentary units that would influence recharge rates to the groundwater.

The study had two specific objectives:

1. To define the principal factors driving variations in electrical conductivity in the sediments of the Riverland region.
2. To ascertain whether the conductive patterns shown in the high frequency apparent conductivity data (eg. 100,000 Hz and 25,000 Hz) and EM inversion products such as conductivity depth imaging (CDI's) and the "Clay Thickness Map" accurately reflect the distribution of clay materials.

These objectives were achieved through targeted drilling, geological logging, the geochemical, mineralogical and petrophysical analysis of bore cuttings and cores, and acquisition of borehole geophysical logs, including conductivity and natural gamma.

3. LOCATION AND HEM DATA ACQUISITION

3.1 Location

Particular focus for the Helicopter EM survey was a 15 - 20 km zone extending away from the southern bank of the river, from Lock 3 near Kingston upon Murray to the Border (Figure 1). Approximately 11,500 line kms of data were acquired. Further details of the data acquisition and processing are provided in the survey Acquisition and Processing Report (Cowey *et al* 2003).

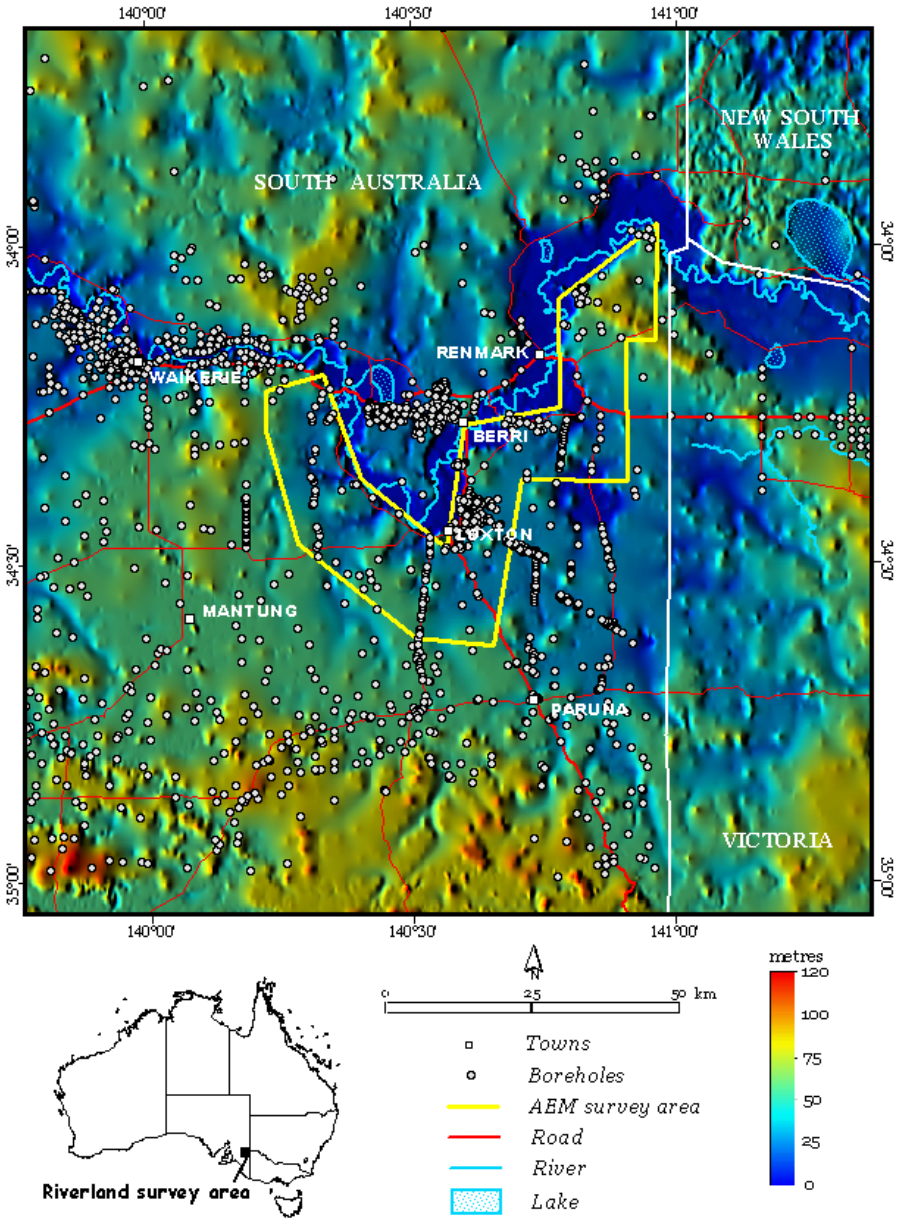

Figure 1. HEM Survey area in the Riverland region of South Australia. Dots represent the locations of exploration boreholes or irrigation bores.

3.2 HEM System

The RESOLVE helicopter electromagnetic (HEM) system is a six frequency EM system that makes use of transmitter and receiver coils housed in a torpedo-shaped tube called a bird that is towed beneath a helicopter. The bird is approximately 10m long and is slung 30 m below the helicopter. During surveying the bird is flown 30 m above the land surface. Using six different frequency-coil-pair combinations, the electromagnetic response is measured as a function of frequency. Data are acquired about every 10 m along flight lines.

Details of the RESOLVE HEM system are summarised in Tables 1 and 2. The RESOLVE bird contains five horizontal coplanar coils, and in the South Australian surveys measured an EM response at 385Hz, 1518Hz, 6135Hz, 25380Hz and 106140 Hz (Table 2), configured as shown in Figure 3. It also has one coaxial coil pair which measured a response at 3323Hz.

Table 1. Summary of RESOLVE HEM system characteristics for the Riverland and Tintinara surveys.

Number of coil sets	6
Navigation	Real time differential GPS mounted on helicopter Ashtech Glonass GG24
Positioning	Post processed GPS mounted on bird Dual-frequency Ashtech Z-Surveyor 1.0 second sample rate
Altimeters	Radar altimeters mounted on helicopter, Sperry RT220 Laser altimeter mounted in bird, Optech G150 0.1 second sample rate
Electromagnetic sampling	6 inphase channels at 0.1 second sample rate 6 quadrature channels at 0.1 second sample rate
Monitor Channels	Horizontal coplanar sferics at 0.1 second sample rate Horizontal coplanar powerline at 0.1 second sample rate Vertical coaxial sferics at 0.1 second sample rate Vertical coaxial powerline at 0.1 second sample rate

Table 2. Summary of RESOLVE coil sets.

Frequency (Hz)	Separation (m)	Orientation	Additive Inphase Noise (Std Dev) Estimate (ppm)	Additive Quadrature Noise (Std Dev) Estimate (ppm)	Multiplicative Inphase Noise (Std Dev) Estimate (%ppm)	Multiplicative Quadrature Noise (Std Dev) Estimate (%ppm)
385	7.86	HCP	2.55	1.5	1.2	1.85
1518	7.86	HCP	4.15	1.9	1.6	2.35
3323	8.99	VCX	2.9	1.5	1.9	2.7
6135	7.86	HCP	5.15	3.2	1.85	2.6
25380	7.86	HCP	8.5	6.65	2.1	2.7
106140	7.86	HCP	13.8	10.4	2.15	2.45

Note: HCP = Horizontal coplanar; VCX = Vertical coaxial

4 GROUND VALIDATION – TARGETED DRILLING

Following the acquisition of the HEM data set, fourteen sites, distributed across the HEM survey area (Figure 2), were selected for coring (Table 3) and soil sampling in late 2002 and early 2003. Four pairs of high and low conductivity sites (numbered 2-5 HC and LC), were selected for coring based upon an analysis of the apparent conductivity images for the 25,000 Hz (Figure 3) and 101 kHz frequencies and a study of available air photos. These paired of sites were typically cored within a kilometre of each other. In addition, high conductivity sites were cored in the northwest (6HC) and southern parts of the study area (3PHC). Following initial review of data from these sites, two more pairs of cores were collected at high and low conductivity sites (7LC, 7HC, 9LC, 9HC).

Bores RIV7HC and RIV7LC were drilled to greater depths (~57 m) so as to provide additional information for the constrained inversion of the HEM data, and to understand causes for an observed conductivity structure noted in the lower frequency apparent conductivity images. Similarly, bores RIV9HC and RIV9LC, which were drilled at a later date when the constrained inversion product – a "clay thickness" image became available. This pair of bore holes was selected to verify an observed discrepancy between the apparent conductivity image and the clay thickness image. The findings are elaborated in sections 5 and 6.

Table 3. Coordinates and depths of the 14 boreholes.

Bore	Easting (mE)	Northing (mN)	Depth (m)
RIV2HC	488601	6226773	15
RIV2LC	487883	6225220	16.5
RIV3PHC	470302	6181008	12
RIV3-1HC	465523	6181208	17.5
RIV3LC	466910	6181580	13
RIV4HC	446586	6190249	16
RIV4LC	447346	6188838	18
RIV5HC	440345	6189981	13
RIV5LC	440033	6189078	16.5
RIV6HC	434795	6205801	16
RIV7HC	453347	6176937	57
RIV7LC	453350	6176000	57
RIV9HC	479856	6198939	33
RIV9LC	479700	6197802	30

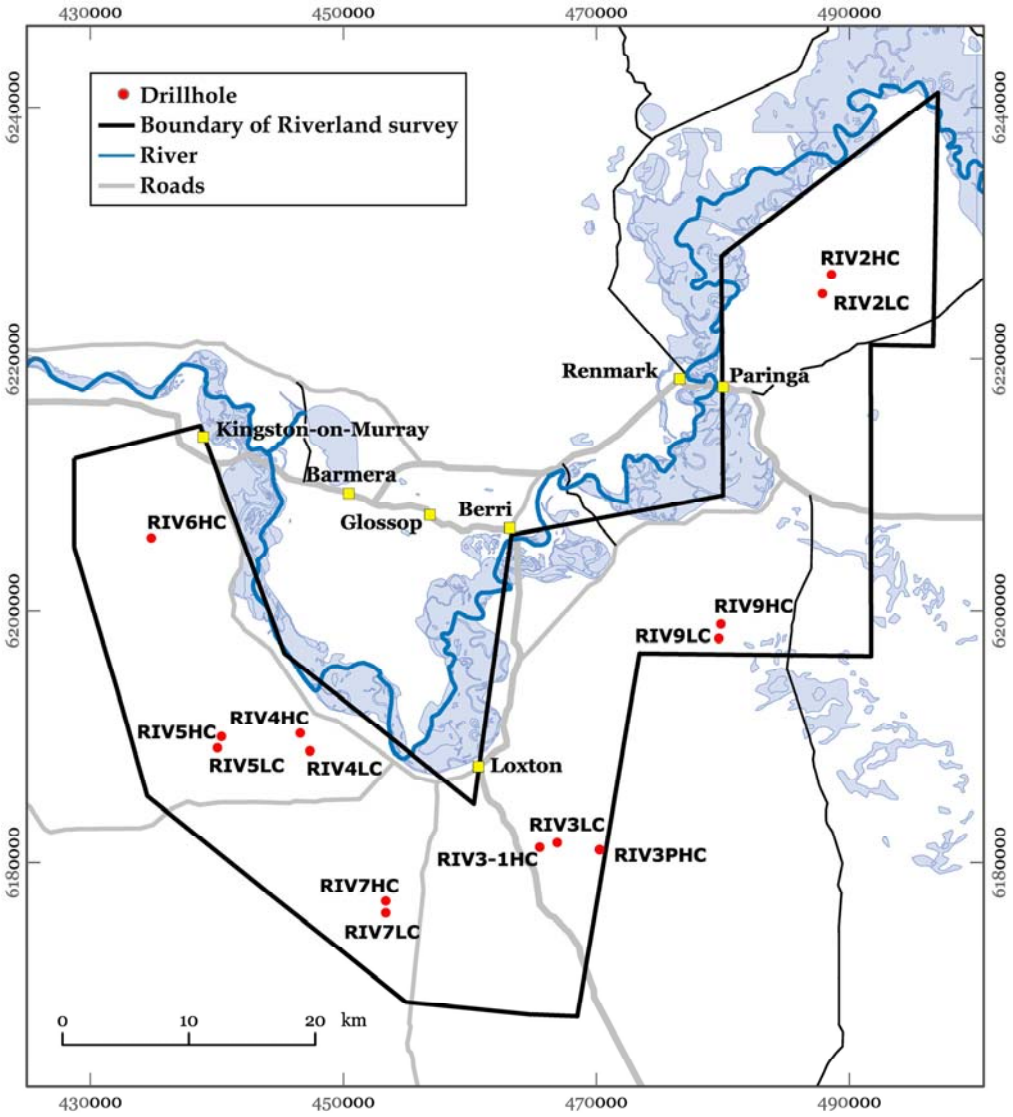

Figure 2. HEM survey area in the Riverland region with the selected location of boreholes examined in this study.

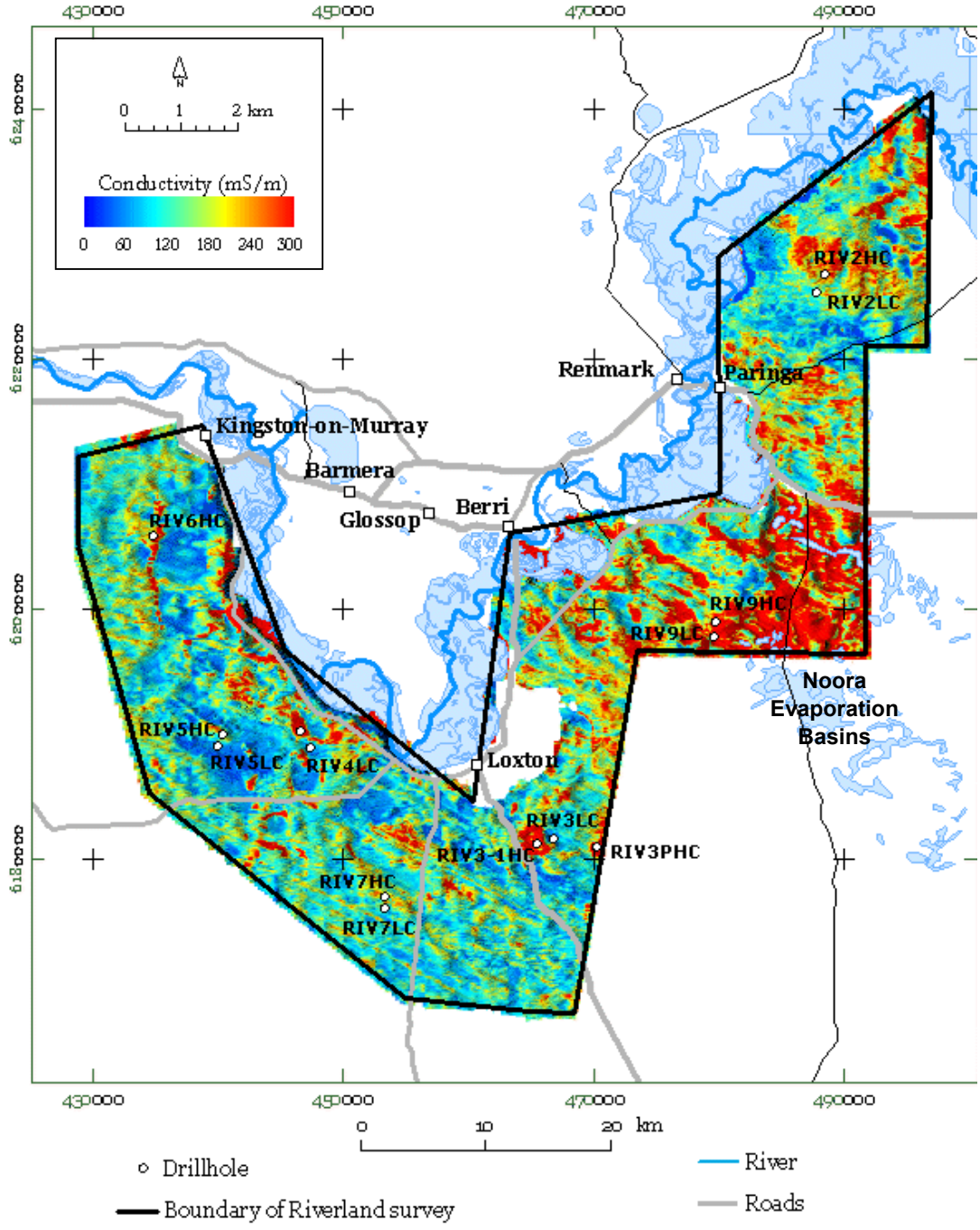

Figure 3. Apparent conductivity image at 25 kHz with the location of boreholes studied here. The conductivity image is draped over a digital elevation image which has an east west sun angle illumination applied.

5. RESULTS

This section illustrates the findings of the petrophysical attributes of samples obtained from the 14 bores. Graphical plots showing the down-hole distribution of water content, Cl concentrations, and down-hole induction and gamma logs are shown in Figures 4 to 17. In addition, information on grain size distribution and mineral composition are tabulated in the appendices.

Several attributes, including sedimentary textures, water content, soil-water Cl concentrations and geophysical logs were measured. Leaney (2000) has described the methods of analysing the gravimetric water content and soil-water Cl. The borehole logs and results derived from the analysis of core were displayed using Logview™ software. Each plot depicts:

- The first column displays the interpreted lithological units. The stratigraphic unit definitions and the lithologic descriptions are elaborated in Brown and Stephenson (1991).
- The second column shows the particle size distribution as sand, silt and clay percentages.
- The third column shows the gravimetric water content of individual samples, with ½ to 1 m composites. The values are in g/g, i.e. weight of water content over weight of wet sample.
- The forth column shows the soil-water chloride concentrations.
- The fifth column displays the apparent electrical conductivity (ECa) measured using the down-hole induction tool.
- The sixth column shows the measured natural gamma response (API) using down-hole natural gamma tool. The response is the composite of emissions of three radioelements K, U and Th and their daughter isotopes.

Down-hole induction and gamma logs were not recorded in bore RIV4HC for logistical reasons.

5.1. Bores RIV2HC and RIV2LC

Bores RIV2HC and RIV2LC are located on elevated dune ridge with elevation up to 90 m AHD at the northeast corner of the survey area. Both bores intersected approximately 3 m of sandy soils with disseminated powdery carbonate and, across a gradual boundary, overlying dominantly massive brown muddy sand (thickness: 9 m for RIV2 HC and 7 m for RIV2 LC). The first 3 m of sandy carbonate soil is interpreted as the Woorinen Formation. The underlying brown muddy sand is strongly ferruginous stained, with higher clay content present locally. This muddy sand is likely to be a palaeosol developed in the Loxton-Parilla Sands, which make up the dune ridge. The fine textured materials of the palaeosol may have an aeolian origin, and is subjected to eluviation in the soil profile. The Woorinen Formation contains moderately to poorly sorted fine to medium sand. The presence of fine-grained carbonates (calcite and dolomite), in addition to kaolinite, gives rise to higher clay and silt abundance. The palaeosol comprises dominantly of medium sand, with smectite, illite and kaolinite locally present (ie. sandy mud). The Loxton-Parilla Sands intersected in bore RIV2HC is dominantly coarse silt and fine sand, whereas those found in RIV2LC comprise dominantly of fine and medium sand.

The down-hole conductivity logs of both bores show “double-peaks”, the first peak occurring from 2-4 m depth at the base of the Woorinen Formation and into the top of the palaeosol, whereas the second peak occurs from 8-10 m depth in the palaeosol. The maximum electrical conductivity (ECa) of the first peak is 320 mS/m for RIV2HC and 305 mS/m for RIV2LC. The ECa of the second peak is 260 mS/m for RIV2HC and 160 mS/m for RIV2LC. Since the ECa of the first peak is similar, the difference in conductivity as observed from the 25,000 Hz image is

attributed to the difference in the second peak (100 mS/m difference), ie. the ECa of the palaeosol. In both bores, the conductivities remain low (50 – 70 mS/m) in the Loxton-Parilla Sands.

5.2. Bore RIV3PHC

Bore RIV3P HC is located at the southern part of the AEM survey area, and the drilling stopped at 12.5 m depth when a lithified / cemented unit was encountered. The lithology intersected includes 4.5 m of brown silty fine sand with carbonate concretions and yellow brown clayey sand, and underlying 8 m of massive, compact to friable, white, buff and pale grey carbonates.

The first unit is interpreted as the Quaternary Woorinen Formation and in addition to the quartz silt and sand, contains white to buff dolomite concretions. The second unit is a dolomite bed (not formally named), and is interpreted as marginal marine carbonate lake deposits similar to the Coorong. These deposits are associated with the Pleistocene strandline (Loxton-Parilla Sands). Quartz and dolomite, with less abundant illite and kaolinite, dominate the top of the dolomite bed, which is dominated by medium silt (20-30 μm). In comparison, the lower part of the dolomite bed comprises clay and very fine silt (< 2 to 4 μm) dominated by dolomite with lesser quartz, mica and kaolinite. The electrical conductivity in the Woorinen Formation is low and increases with depth in the dolomite bed.

5.3. Bore RIV3-1HC

This bore is located at the foot slope of a Pleistocene dune and intersected 4 distinct lithological units. The top 3.4 m consists of brown, friable, dominantly fine sand to muddy sand with carbonates cement commonly 10 to 20 cm thick. Carbonate concretions and earthy fine-grained carbonates are also present. This unit is interpreted as the Woorinen Formation. Underlying is 1.6 m of white layered carbonates and brown clayey sand interbeds interpreted as the Bungunnia Limestone. Underlying is 6 m of massive and dense, light to medium grey sandy mud. Grain size distribution shows that fine sand and silt dominates the texture, with the latter associated with increasing smectite, kaolinite and illite contents. This unit is interpreted as the Blanchetown Clay, which overlies, across a sharp contact, at least 6 m of massive, white, partly friable, fine-grained dolomite bed, similar to those found in bore RIV3PHC.

The conductivity log shows double peaks, the first occurs from 4-6 m in the Bungunnia Limestone and the top of Blanchetown Clay, and the second peak is from 8-10 m in the Blanchetown Clay. Overall, the gravimetric water content is low in the Woorinen Formation, whereas the Bungunnia Limestone and Blanchetown Clay has higher but heterogenous water content. In comparison, the dolomite bed has moderate but consistent (0.2-0.3 g/g) water content. Soil-water Cl is low in the Woorinen Formation, but increases in the Bungunnia Limestone and remains constant (average 22,000 mg/l) in the Blanchetown Clay, and increases again in the dolomite bed (average 23,000 mg/l).

5.4. Bore RIV3LC

Borehole RIV3LC intersected 3.3 m of brown fine sandy soil with yellow and buff carbonate occurring as hard bands. This unit is interpreted as the Woorinen Formation. Underlying is at

least 10.5 m of pale yellow brown to yellow brown, massive, dominantly moderately sorted fine to medium sand, interpreted as the Loxton-Parilla Sands. From 8 to 13.5 m (end of hole) is the presence of graded beds, which alternate between bimodal, poorly sorted, fine to very coarse sand (and granules) and moderately sorted fine to medium sand. Muscovite is locally present, and is more abundant in the coarse sand beds.

The apparent conductivity response remains low throughout the Loxton-Parilla Sands, accompanied by low water content (<0.1 to 0.2 g/g) and high soil-water Cl (10,000 to 20,000 mg/l). The apparent conductivity increases sharply (1,000 mS/m) at the water table (at 13 m depth).

5.5. Bore RIV4HC

Three lithologic units are present in bore RIV4HC. The top unit comprises 4.5 m of brown muddy fine sand and fine to medium sand with strong carbonate (calcite, dolomite) development. Underlying is 3.5 m of stiff brown and grey clay. The former unit is interpreted as the Woorinen Formation whereas the latter is the Blanchetown Clay, which overlies at least 9 m of yellow, pale brown, fine to medium sand with interbeds of poorly sorted medium to coarse sand.

The water content for the Woorinen Formation is low (0.1 g/g), whereas those of Blanchetown Clay is high (0.3 – 0.4 g/g). Apart from a moderately moist interval (1 m) at the top, the remaining Loxton-Parilla Sands have low water content (< 0.05 g/g). Salinity of the pore fluid is low at the surface, but reaches 18,000 mg/l at 3 m depth and remains consistent throughout the Blanchetown Clay and Loxton-Parilla Sands.

5.6. Bore RIV4LC

Bore RIV4LC intersected 3 distinct lithological units. The first 4 m consists of friable, brown, poorly sorted fine to coarse sand and silt with massive carbonate. This unit is interpreted as the Woorinen Formation. Underlying is 12.5 m of sand, with texture comprises well-sorted fine sand, poorly sorted fine to very coarse sand and bimodal fine sand and granules. This unit is interpreted as the Loxton-Parilla Sand. A thin band (20 cm) of dark resistate minerals at 6.2 m gives rise to local high gamma response (> 100 API). Underlying is at least 1.5 m (16.5-18 m depths) of massive calcarenite with gastropod fossils (Turritella). This unit is interpreted as the Murray Group Limestone.

The electrical conductivities and the water contents remain relatively low and consistent throughout the Woorinen Formation and the Loxton-Parilla Sands (150-200 mS/m and 0.1-0.2 g/g respectively). The Cl concentrations in both the Woorinen Formation and the Loxton-Parilla Sands range from 10,000 to 20,000 mg/l.

5.7. Bore RIV5HC

Borehole RIV5HC was located on Pleistocene dune, and intersected 4 m of massive, brown, fine to medium sand. Apart from the near surface ploughed sandy soil, variegated, massive and cemented carbonate is present from 0.4 m depth. This unit is interpreted as the Woorinen Formation. Underlying is 2.5 m of massive, dominantly white, fine grained (clay and silt), mostly

cemented carbonate (dolomite) and is interpreted to be the Bungunnia Limestone. This unit overlies 3.3 m of variegated (buff, white and light grey) silt with minor sand layer, interpreted as the Blanchetown Clay. Underlying is at least 3.3 m of massive, yellow to yellow brown well-sorted fine sand, which is interpreted as the Loxton-Parilla Sands.

The water content is low (0.1-0.2 g/g) in the Woorinen Formation, but increases in the Bungunnia Limestone and Blanchetown Clay, and decreases in the Loxton-Parilla Sands (0.1 g/g). The Cl concentrations are low in the Woorinen Formation, increase in the Bungunnia Limestone and Blanchetown Clay, and remain constant in the Loxton-Parilla Sands. The apparent conductivity is high for the Bungunnia Limestone and the Blanchetown Clay but low for both the Woorinen Formation and Loxton-Parilla Sands.

5.8. Bore RIV5LC

Borehole RIV5LC intersected 2 m of brown fine sandy soil with buff, massive to cemented carbonates. This unit is interpreted as the Woorinen Formation. Underlying is 10.9 m of massive, unconsolidated to compact, dominantly fine to medium sand. Weathering and diagenesis have produced localised carbonate cemented sand, and zones of yellow/brown Fe-oxide coated and leached sand. The unit also contains scattered dark heavy minerals and muscovite. This unit is postulated to be the Loxton-Parilla Sands. Underlying is at least 3.6 m of white to buff lithified / cemented to friable carbonate with gastropod fossils and this unit is interpreted to be the Miocene Murray Group Limestone.

No down-hole conductivity and gamma log data is available below 13.3 m due to the collapsed of the sand and limestone, but the available conductivity data shows that the Loxton-Parilla Sands has low conductivity (average 100 mS/m). The gravimetric water content remains low (0.1-0.2 g/g) whereas the Cl concentrations are high (> 20,000 mg/l).

5.9. Bore RIV6 HC

Borehole RIV6HC intersected 2 m of loose, light yellow-brown, well-sorted fine sand. Underlying is 3 m of massive compact, light brown, fine to medium sand. This overlies 2 m of buff to light brown, massive and compact fine to medium quartz sand with lesser silt. The unit is cemented in places by carbonate, and appears buff when abundant massive carbonate is present. Underlying is 4 m (ie. 7 – 11 m depth) of buff, light grey and red-brown muddy sand with Fe-oxide and carbonate segregation. The clayey sand increases in Fe-oxide abundance (becomes strong brown) but decreases in carbonate contents with depth. Muscovite is present in this unit. Underlying is at least 6 m of light grey to light brown with local ferruginous (brown) fine to medium sand.

The top 7 m of combined loose to compact, fine to medium sand and the carbonate are interpreted as the Woorinen Formation. The underlying 4 m of Fe-oxide segregated (ie. mottled) clayey sand is assigned as the Blanchetown Clay, whereas the underlying 6 m of fine to medium sand is interpreted as the Loxton-Parilla Sands.

The gravimetric water content is low in the Woorinen Sand, increases in the buff carbonate silty sand, and peaked in the Blanchetown Clay (0.18 g/g or 18 %), and remains consistent in the Loxton-Parilla Sands (average 0.1 g/g). In comparison, the soil-water Cl is low in both the Woorinen Sand and buff carbonate sand, and increases in the Loxton-Parilla Sands. The apparent

conductivity is low (50 mS/m) for the Woorinen Formation, and a high conductivity (average 250 mS/m) for the Blanchetown clay (clayey sand) and the Loxton-Parilla Sands.

5.10 RIV7HC

The top 3 m comprises brown, well sorted fine sand and moderately sorted fine to medium sand with fragments of cemented carbonate. This unit is interpreted as the Woorinen Formation. Underlying is 4 m of yellow brown sandy clay and clayey sand with an elevated conductivity of up to 400 mS/m. This unit is interpreted to be the Blanchetown Clay. Underlying is 25 m (ie. to 32 m depth) of dry, yellow to dark yellow, well-sorted fine sand with minor beds of coarse sand interpreted to be the Loxton-Parilla Sands. From 32 m depth is 9 m of pale grey, cemented limestone (calcarenite) with gastropod casts preserved in cemented drill cuttings. This is underlain by 16 m of medium grey fine sandy clay with varying abundance of cemented limestone (calcilutite). XRD analysis shows that the calcarenite is dominantly calcite with minor quartz, whereas the calcilutite comprises dominantly calcite, and lesser abundance of aragonite, quartz, illite and kaolinite. Both the calcarenite and calcilutite are interpreted to be part of the Murray Group Limestone. The down hole conductivity log stopped at 41 m in the grey clay due to collapse of the sidewall. Nevertheless, the 4 m of saturated calcilutite gives high conductivity values (between 800 to 900 mS/m).

5.11 RIV7LC

The top metre comprises of poorly sorted fine to coarse sand interpreted as the Woorinen Formation. Underlying is 3 m of brown, moderately sorted fine to medium sand and sandy clay. This unit is interpreted as the Blanchetown Clay. The apparent conductivity increases from 2 to 4 m depths corresponding to an increase in the clay content. Underlying is 19 m of yellow, moderately to poorly sorted sand (fine to medium for the former and fine to very coarse and granules for the latter). This unit is interpreted as the Loxton-Parilla Sands. Underlying (at 23 m depth) is yellow brown to khaki, carbonate bearing, variably cemented calcarenite. Highly cemented calcarenite is present between 30 to 32 m, which corresponds to a low conductivity value of less than 50 mS/m. A redox boundary is present at 40 m depth when the calcarenite changes from dark yellow to olive grey/medium grey. Shell fragments have been observed in the cemented calcarenite. XRD analysis shows that the calcarenite is dominated by calcite, with lesser aragonite and traces of quartz and ankerite. This calcarenite sequence is interpreted as the Murray Group Limestone.

The downhole conductivity log suggests that the conductivity of the calcarenite ranges from 150 to 220 mS/m, with low conductivity of approximately 50 mS/m associated with highly cemented carbonate, and up to 300 mS/m associated with abundant fine carbonate sand and clay (calcilutite).

5.12 RIV9HC

The bores RIV9HC intersected top 4 m of brown moderately sorted fine to medium sand with cemented carbonates, interpreted as the Woorinen Formation. Underlying is 4 m of brown sandy clay and 8 m of olive grey clay-rich sediments, interpreted to be the Blanchetown Clay. These

clay-rich sediments (up to 83 % clay, comprising of kaolinite) have conductivity values reaching above 1,000 mS/m.

Underlying the Blanchetown Clay is 9 m of yellow brown well-sorted fine or medium sand, and moderately sorted fine to medium sand. Water table was intersected at 22 m depth in the yellow brown sand. At least 7 m of olive grey to dark grey, moderately to poorly sorted sand underlies the brown sand, and the colour varies from yellow brown to grey indicates a change towards reducing conditions. The lower fine sand unit is interpreted as the lower Loxton Sands (shallow marine facies). The unsaturated sand has low conductivity (< 50 mS/m) whereas the saturated sand has high conductivity (800 to 1,000 mS/m).

5.13 RIV9LC

Bore RIV9LC was carried out at a lower elevation than RIV9HC and intersected the water table at 8 m depth. The top metre consists of Holocene dune sand, which blanket 3 m of poorly sorted fine to coarse sand with calcrete, infer as the Woorinen Formation. Underlying is 8 m of yellow to brown, poorly sorted fine to coarse sand, followed by 2 m of grey quartz sand. This unit is interpreted as the Loxton-Parilla Sands, which overlies at least 18 m of interbedded dark grey sand. The beds include fine to medium and medium to coarse sand, with abundant dark green glauconitic grains. XRD analysis of this unit shows abundant quartz and glauconite, with lesser calcite and trace aragonite, and this unit is interpreted as the lower Loxton Sands (marine facies).

The down-hole conductivity log stopped at 12 m depth due to the collapsed of the saturated sand. Nevertheless, the result shows that the unsaturated Loxton-Parilla Sands produces low conductivity values (approximately 50 mS/m) whereas the saturated Loxton-Parilla Sands and the Lower Loxton Sand have high conductivity values (>1000 mS/m), and the presence of highly saline groundwater (30,000 to > 60,000 mg/l Cl).

Bore RIV2HC

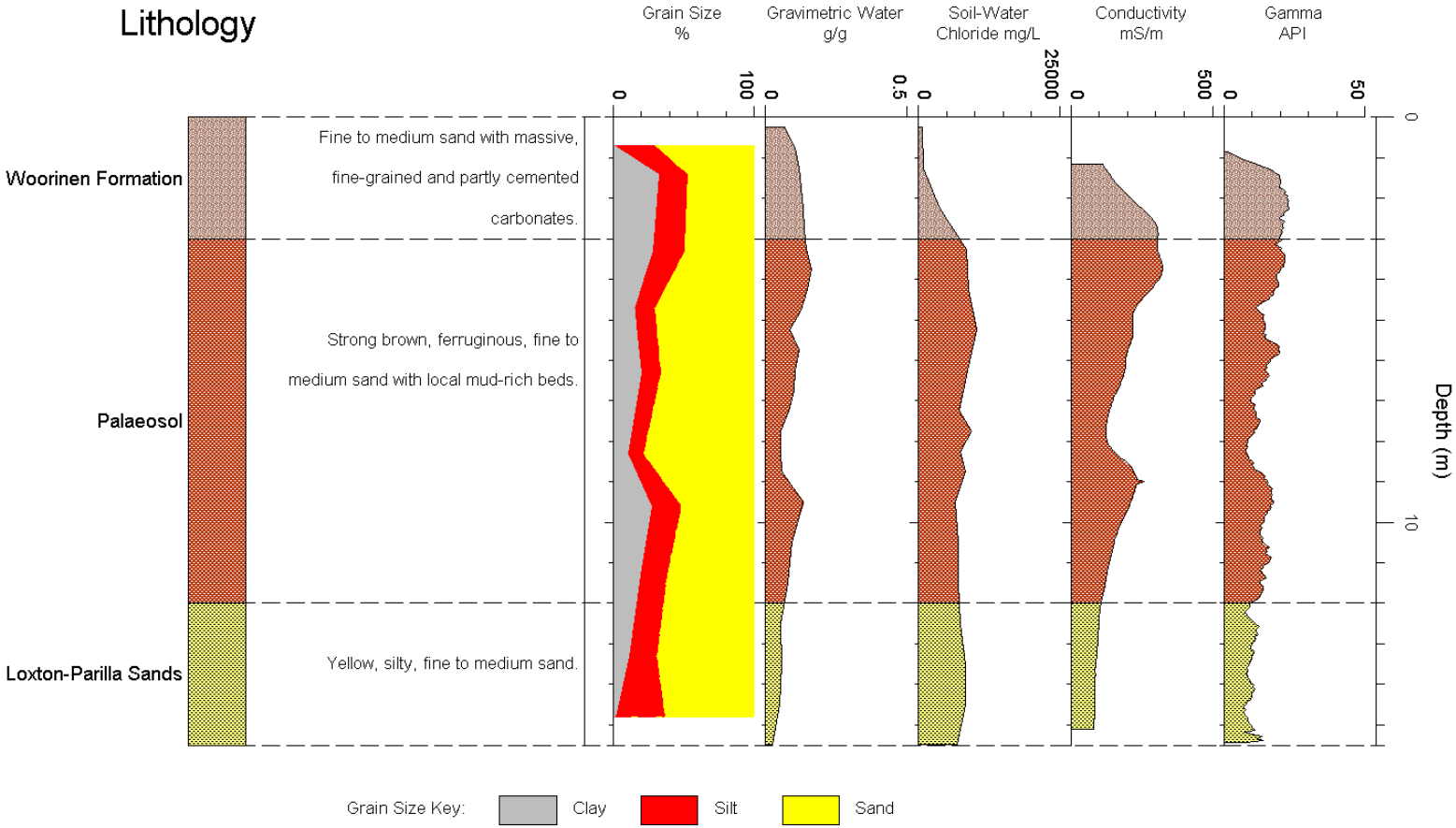
Lithology
Grain Size
%
Gravimetric Water
g/g
Soil-Water
Chloride mg/L
Conductivity
mS/m
Gamma
API
0
100
0
0.5
0
25000
0
500
0
50
Woorinen Formation
Fine to medium sand with massive, fine-grained and partly cemented carbonates.
Palaeosol
Strong brown, ferruginous, fine to medium sand with local mud-rich beds.
Loxton-Parilla Sands
Yellow, silty, fine to medium sand.
Depth (m)
0
10
Grain Size Key:
Clay
Silt
Sand

Bore RIV2LC

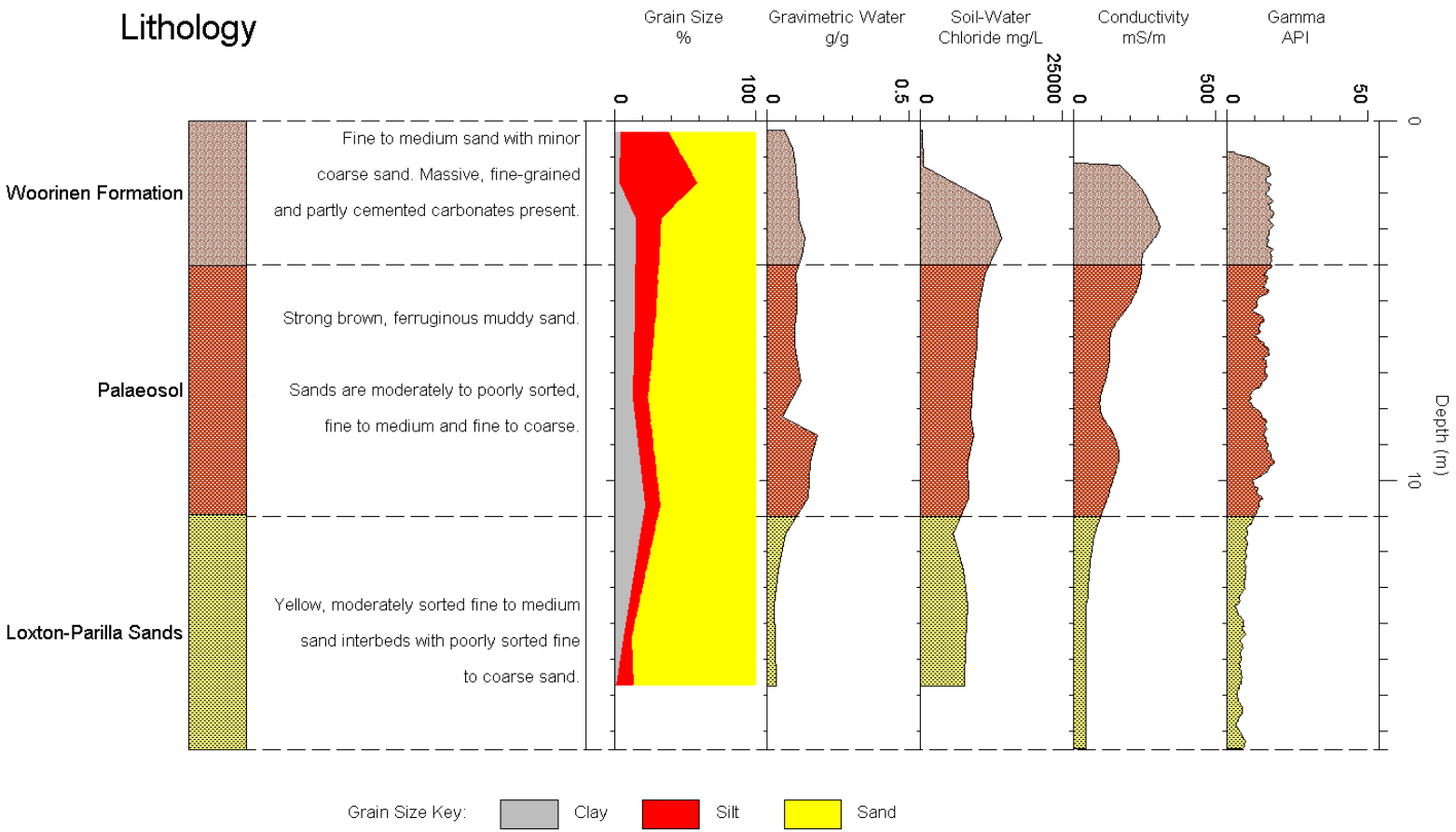
Lithology
Grain Size %
Gravimetric Water g/g
Soil-Water Chloride mg/L
Conductivity mS/m
Gamma API
0
100
0
0.5
0
25000
0
500
0
50
Woorinen Formation
Fine to medium sand with minor coarse sand. Massive, fine-grained and partly cemented carbonates present.
Palaeosol
Strong brown, ferruginous muddy sand.
Sands are moderately to poorly sorted, fine to medium and fine to coarse.
Loxton-Parilla Sands
Yellow, moderately sorted fine to medium sand interbeds with poorly sorted fine to coarse sand.
Depth (m)
0
10
Grain Size Key:
Clay
Silt
Sand

Bore RIV3P-HC

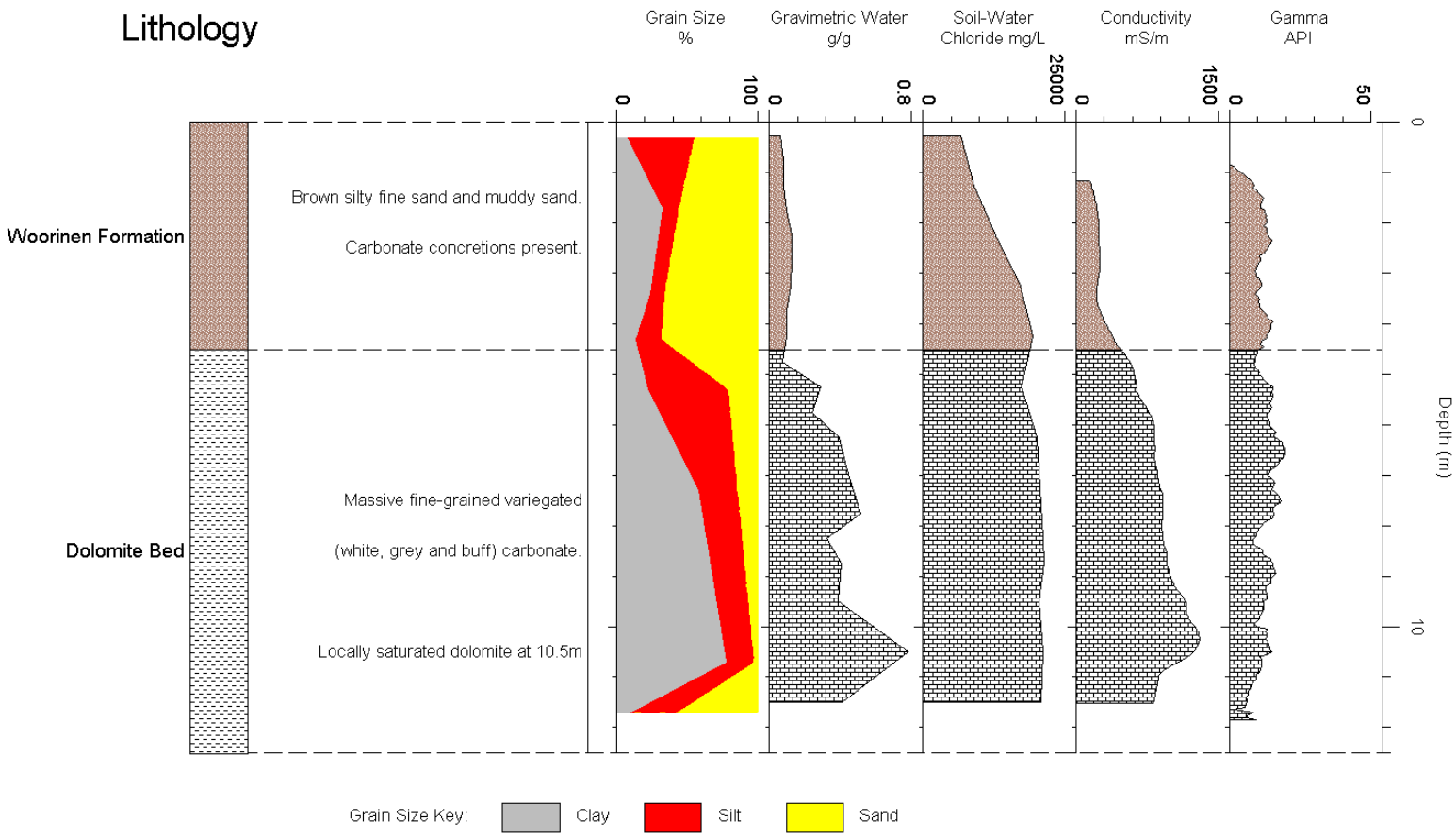

Bore RIV3-1HC

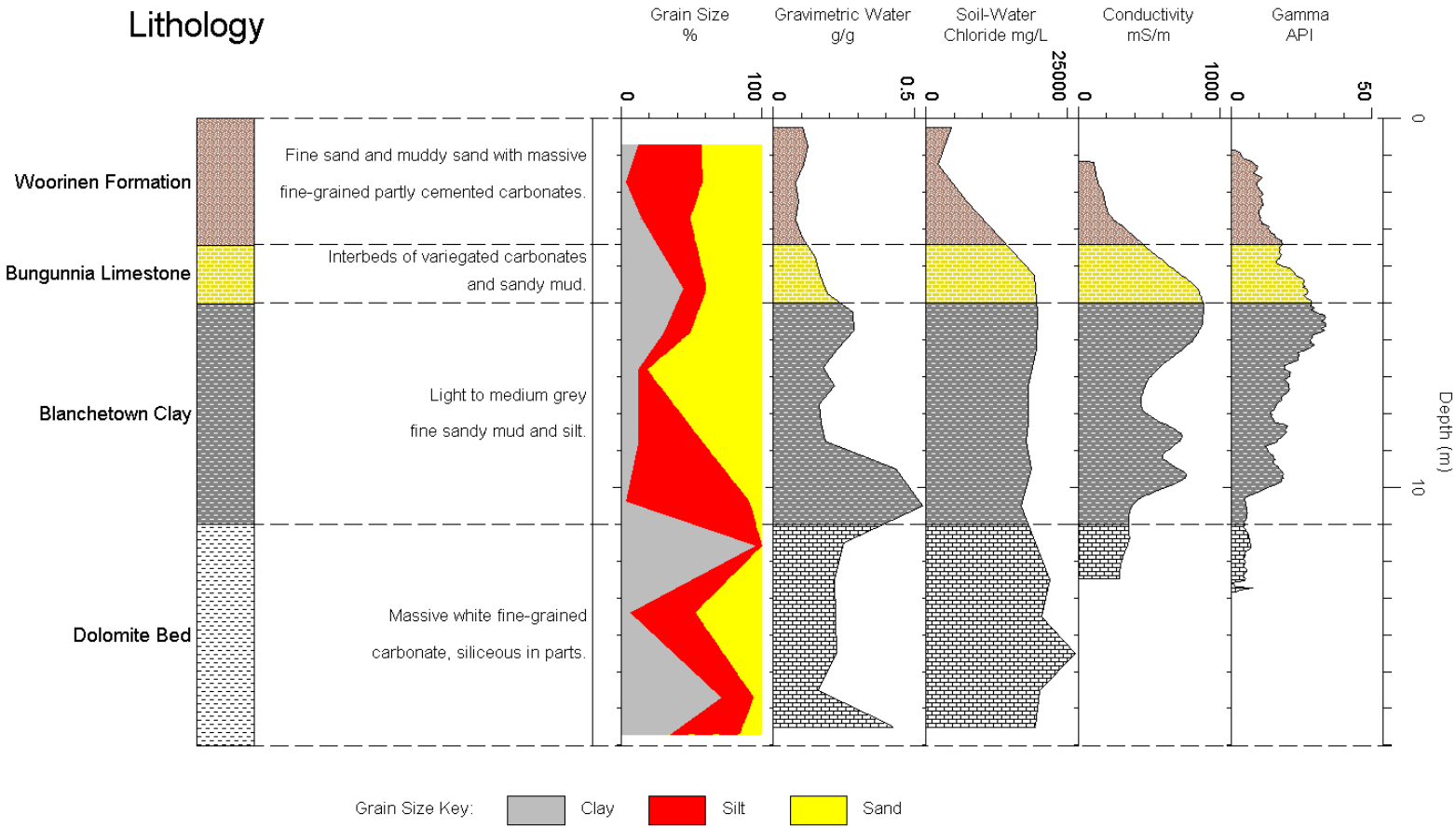

Bore RIV3LC

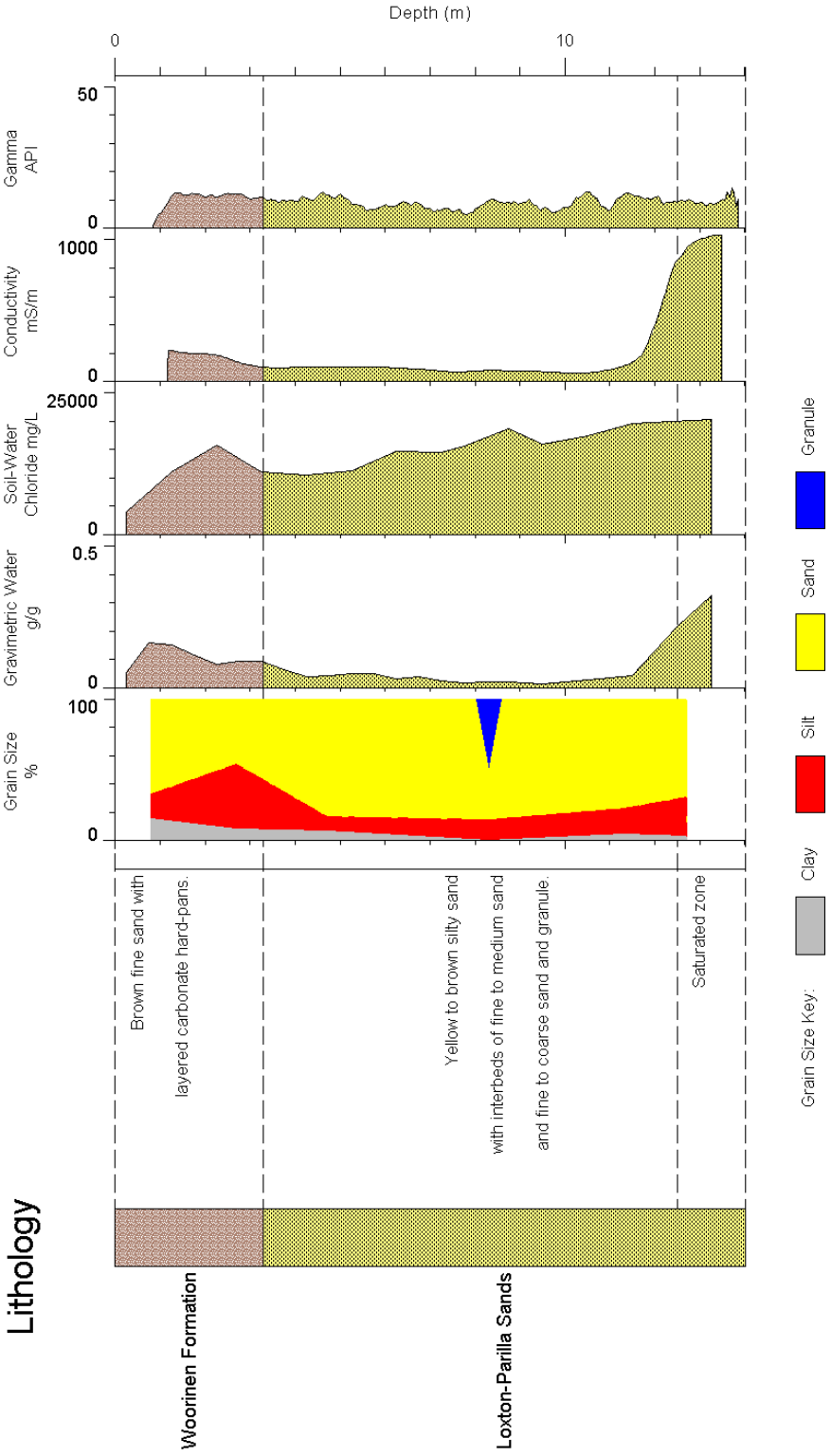
Depth (m)
0
10
Gamma API
50
0
Conductivity mS/m
1000
0
Soil-Water Chloride mg/L
25000
0
Gravimetric Water g/g
0.5
0
Grain Size %
100
0
Lithology
Brown fine sand with layered carbonate hard-pans.
Yellow to brown silty sand with interbeds of fine to medium sand and fine to coarse sand and granule.
Saturated zone
Woorinen Formation
Loxton-Parilla Sands
Grain Size Key:
Clay
Silt
Sand
Granule

Bore RIV4HC

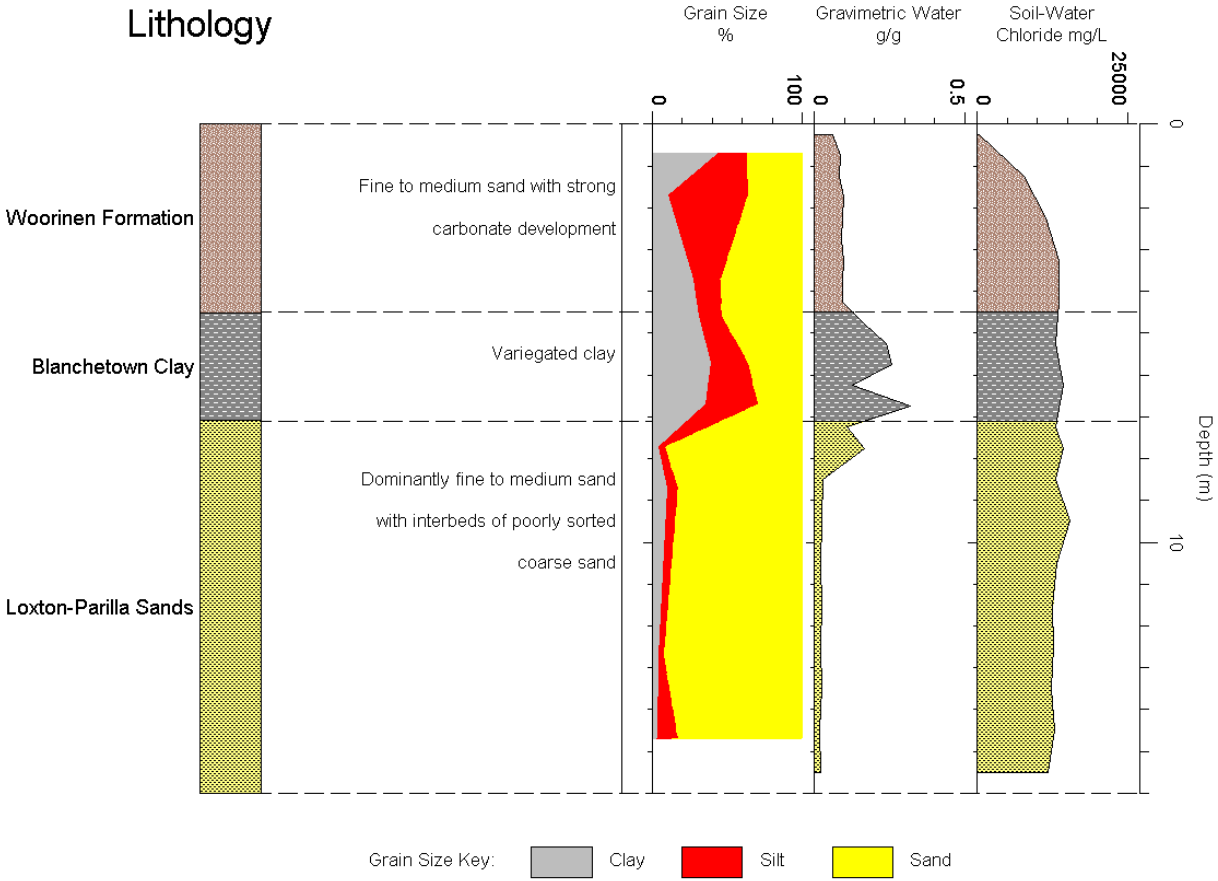
Lithology
Grain Size
%
Gravimetric Water
g/g
Soil-Water
Chloride mg/L
0
100
0
0.5
0
25000
0
10
Depth (m)
Woorinen Formation
Blanchetown Clay
Loxton-Parilla Sands
Fine to medium sand with strong
carbonate development
Variegated clay
Dominantly fine to medium sand
with interbeds of poorly sorted
coarse sand
Grain Size Key:
Clay
Silt
Sand

Bore RIV4LC

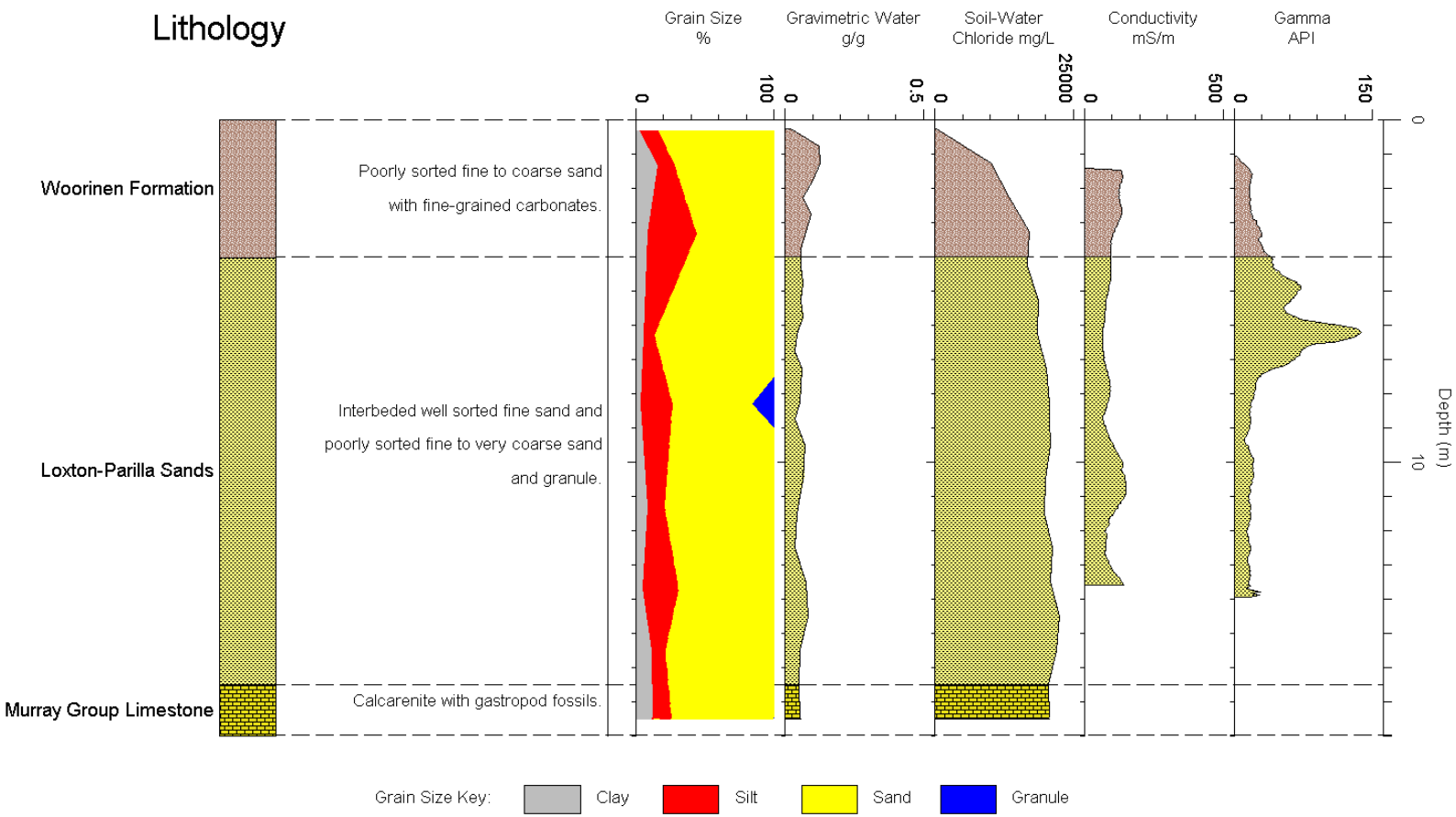
Lithology
Grain Size
%
Gravimetric Water
g/g
Soil-Water
Chloride mg/L
Conductivity
mS/m
Gamma
API
0
100
0
0.5
0
25000
0
500
0
150
Woorinen Formation
Poorly sorted fine to coarse sand
with fine-grained carbonates.
Loxton-Parilla Sands
Interbeded well sorted fine sand and
poorly sorted fine to very coarse sand
and granule.
Murray Group Limestone
Calcarenite with gastropod fossils.
Depth (m)
0
10
Grain Size Key:
Clay
Silt
Sand
Granule

Bore RIV5HC

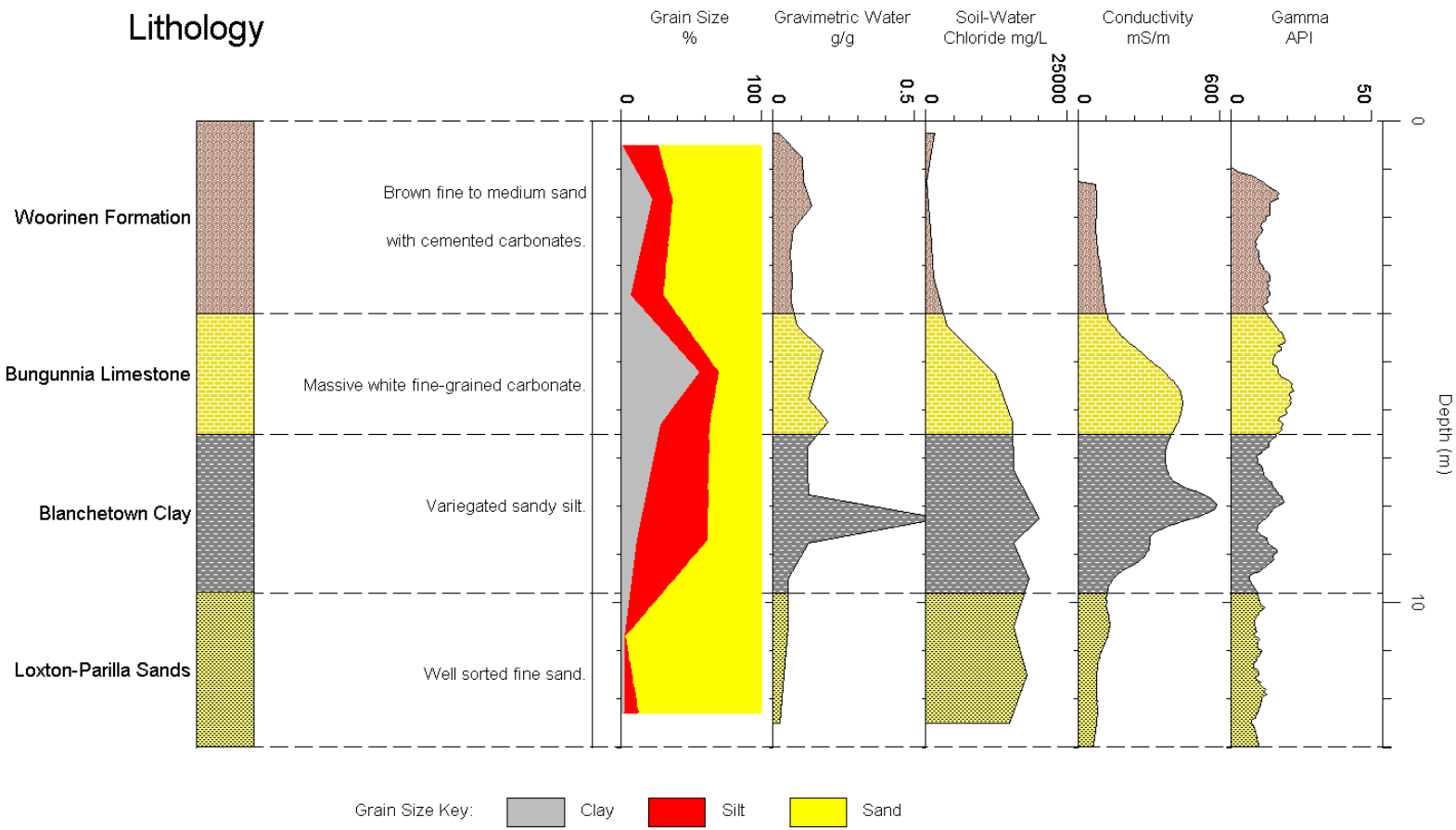
Lithology
Grain Size
%
Gravimetric Water
g/g
Soil-Water
Chloride mg/L
Conductivity
mS/m
Gamma
API
0
100
0
0.5
0
25000
0
600
0
50
0
10
Depth (m)
Woorinen Formation
Brown fine to medium sand
with cemented carbonates.
Bungunnia Limestone
Massive white fine-grained carbonate.
Blanchetown Clay
Variegated sandy silt.
Loxton-Parilla Sands
Well sorted fine sand.
Grain Size Key:
Clay
Silt
Sand

Bore RIV5LC

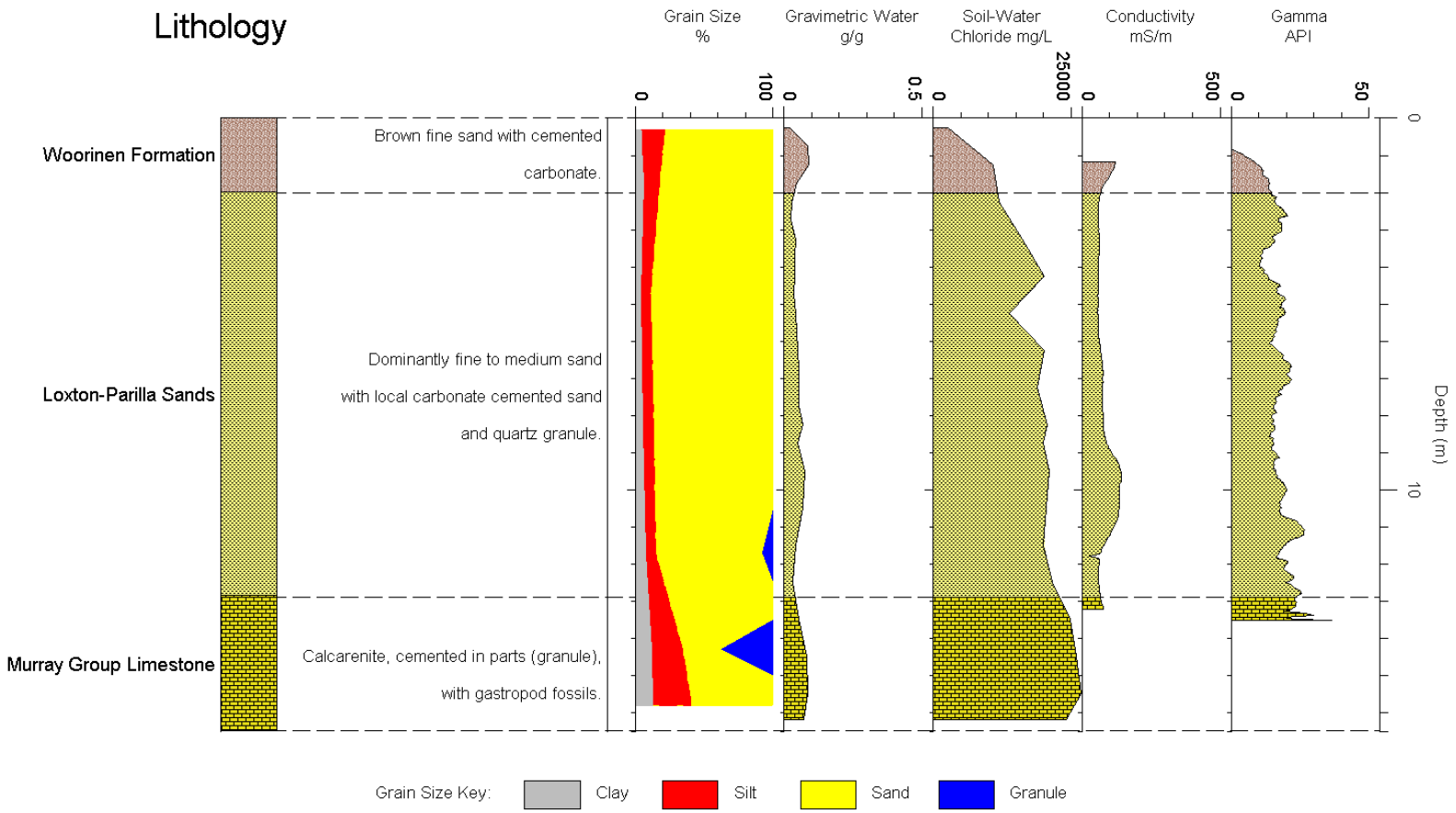
Lithology
Grain Size %
Gravimetric Water g/g
Soil-Water Chloride mg/L
Conductivity mS/m
Gamma API
0
100
0
0.5
0
25000
0
500
0
50
0
10
Depth (m)
Woorinen Formation
Brown fine sand with cemented carbonate.
Loxton-Parilla Sands
Dominantly fine to medium sand with local carbonate cemented sand and quartz granule.
Murray Group Limestone
Calcarenite, cemented in parts (granule), with gastropod fossils.
Grain Size Key:
Clay
Silt
Sand
Granule

Bore RIV6HC

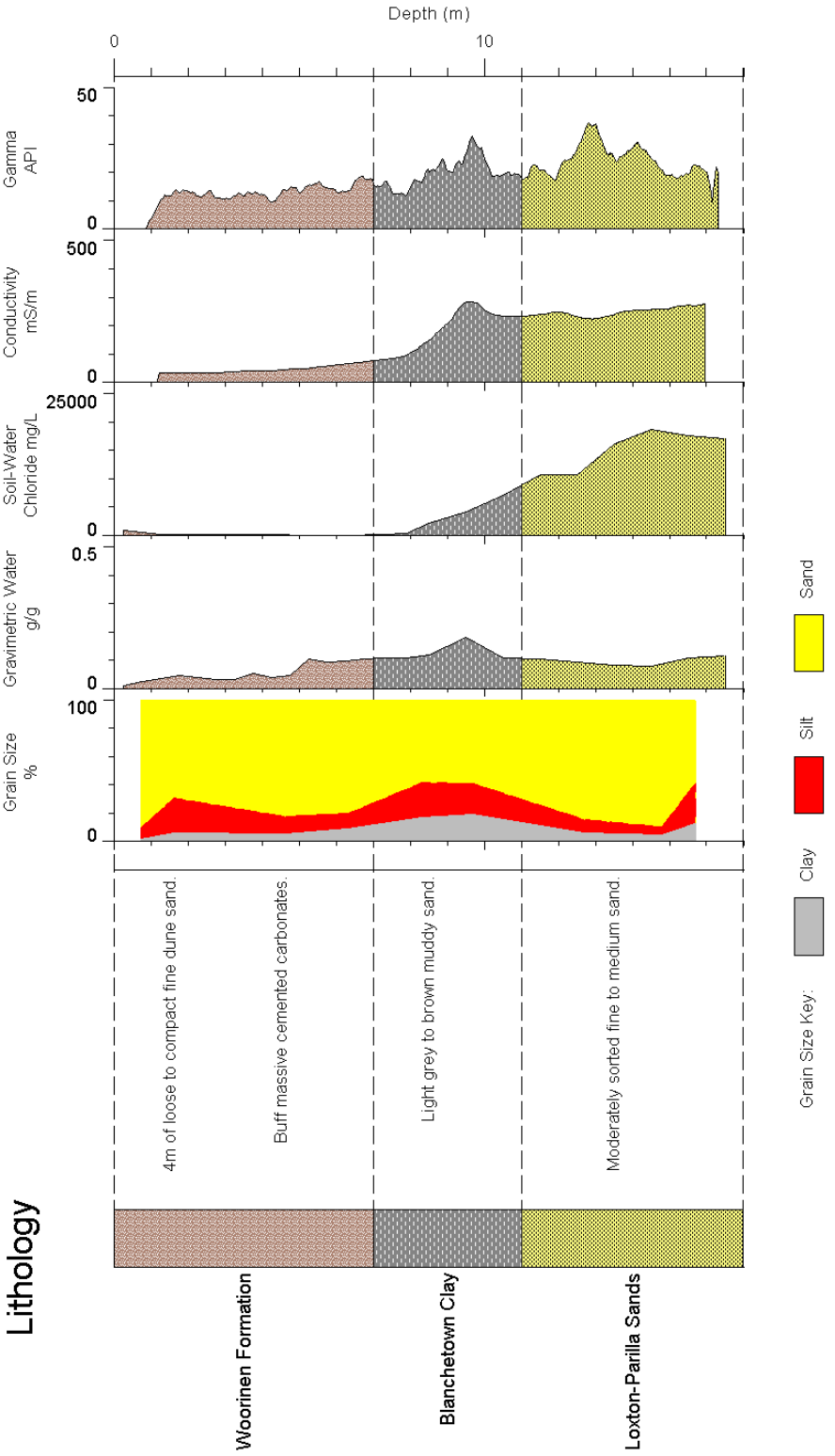
Depth (m)
0
10
Gamma API
50
0
Conductivity mS/m
500
0
Soil-Water Chloride mg/L
25000
0
Gravimetric Water g/g
0.5
0
Grain Size %
100
0
Lithology
4m of loose to compact fine dune sand.
Buff massive cemented carbonates.
Light grey to brown muddy sand.
Moderately sorted fine to medium sand.
Woorinen Formation
Blanchetown Clay
Loxton-Parilla Sands
Grain Size Key:
Clay
Silt
Sand

Bore RIV7HC

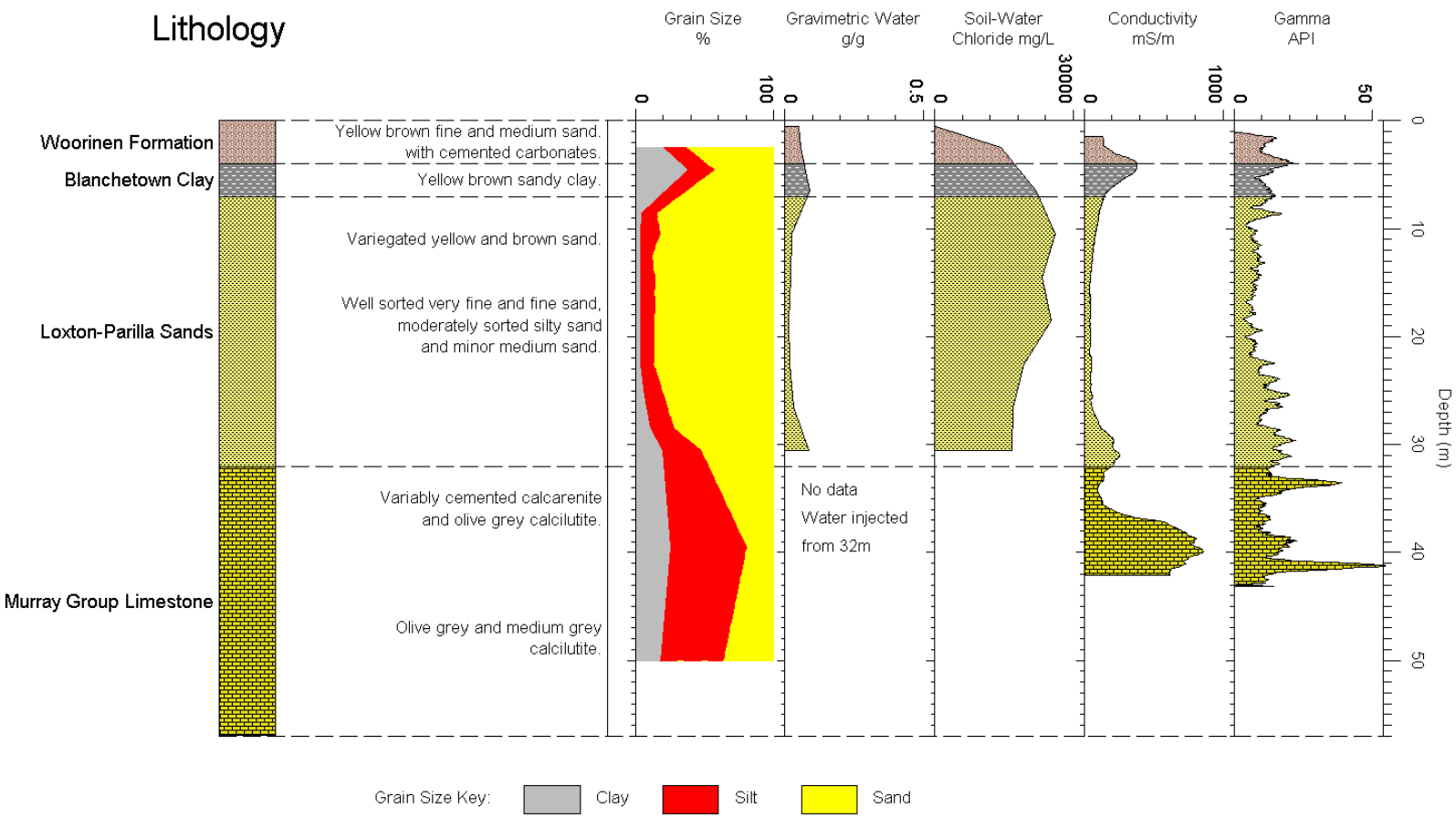
Lithology
Grain Size %
Gravimetric Water g/g
Soil-Water Chloride mg/L
Conductivity mS/m
Gamma API
0
100
0
0.5
0
30000
0
1000
0
50
Woorinen Formation
Blanchetown Clay
Loxton-Parilla Sands
Murray Group Limestone
Yellow brown fine and medium sand. with cemented carbonates.
Yellow brown sandy clay.
Variegated yellow and brown sand.
Well sorted very fine and fine sand, moderately sorted silty sand and minor medium sand.
Variably cemented calcarenite and olive grey calcilutite.
Olive grey and medium grey calcilutite.
No data
Water injected
from 32m
0
10
20
30
40
50
Depth (m)
Grain Size Key:
Clay
Silt
Sand

Bore RIV7LC

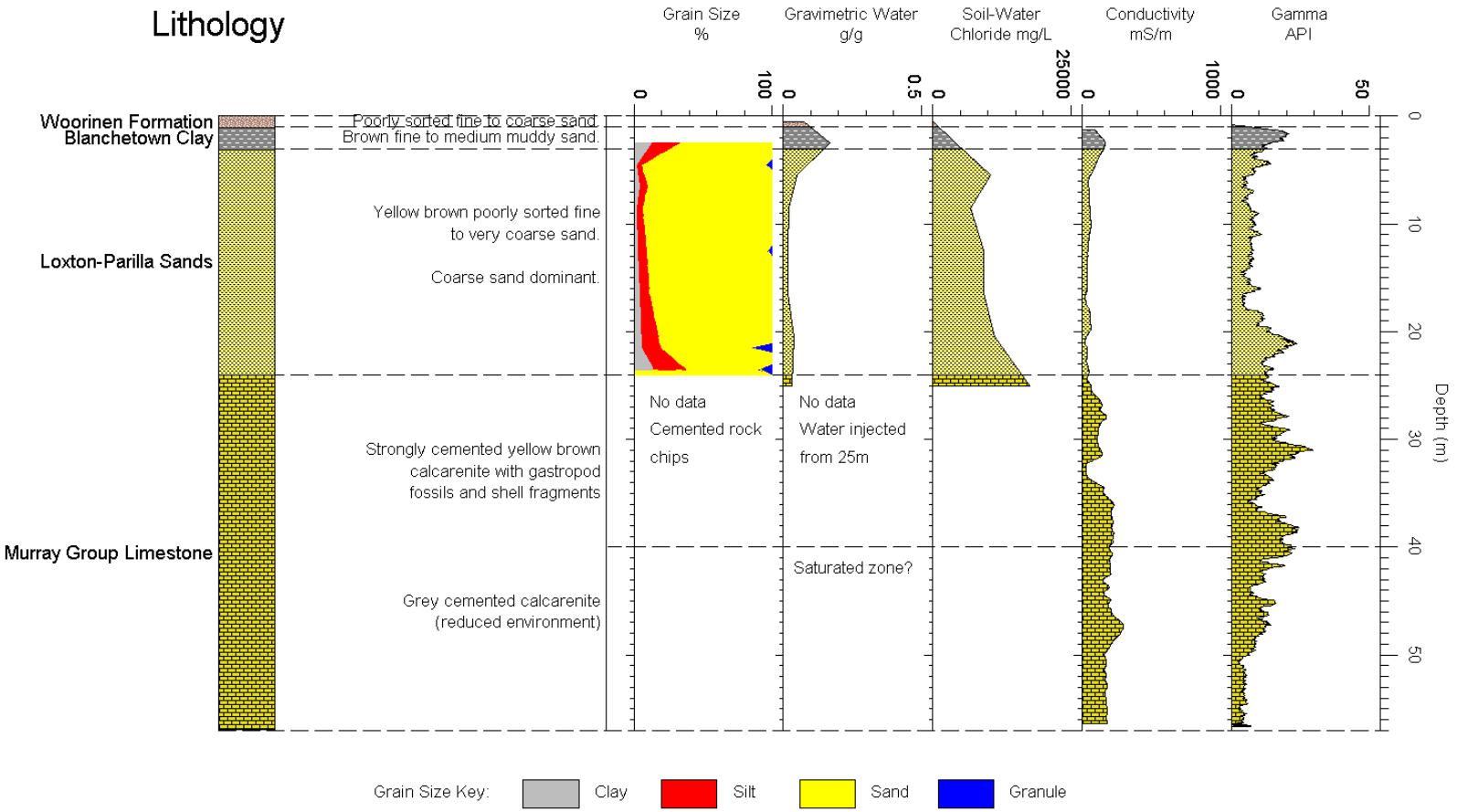
Lithology
Grain Size %
Gravimetric Water g/g
Soil-Water Chloride mg/L
Conductivity mS/m
Gamma API
0
100
0
0.5
0
25000
0
1000
0
50
Woorinen Formation
Blanchetown Clay
Loxton-Parilla Sands
Murray Group Limestone
Poorly sorted fine to coarse sand.
Brown fine to medium muddy sand.
Yellow brown poorly sorted fine to very coarse sand.
Coarse sand dominant.
Strongly cemented yellow brown calcarenite with gastropod fossils and shell fragments
Grey cemented calcarenite (reduced environment)
No data
Cemented rock chips
No data
Water injected from 25m
Saturated zone?
Depth (m)
0
10
20
30
40
50
Grain Size Key:
Clay
Silt
Sand
Granule

Bore RIV9HC

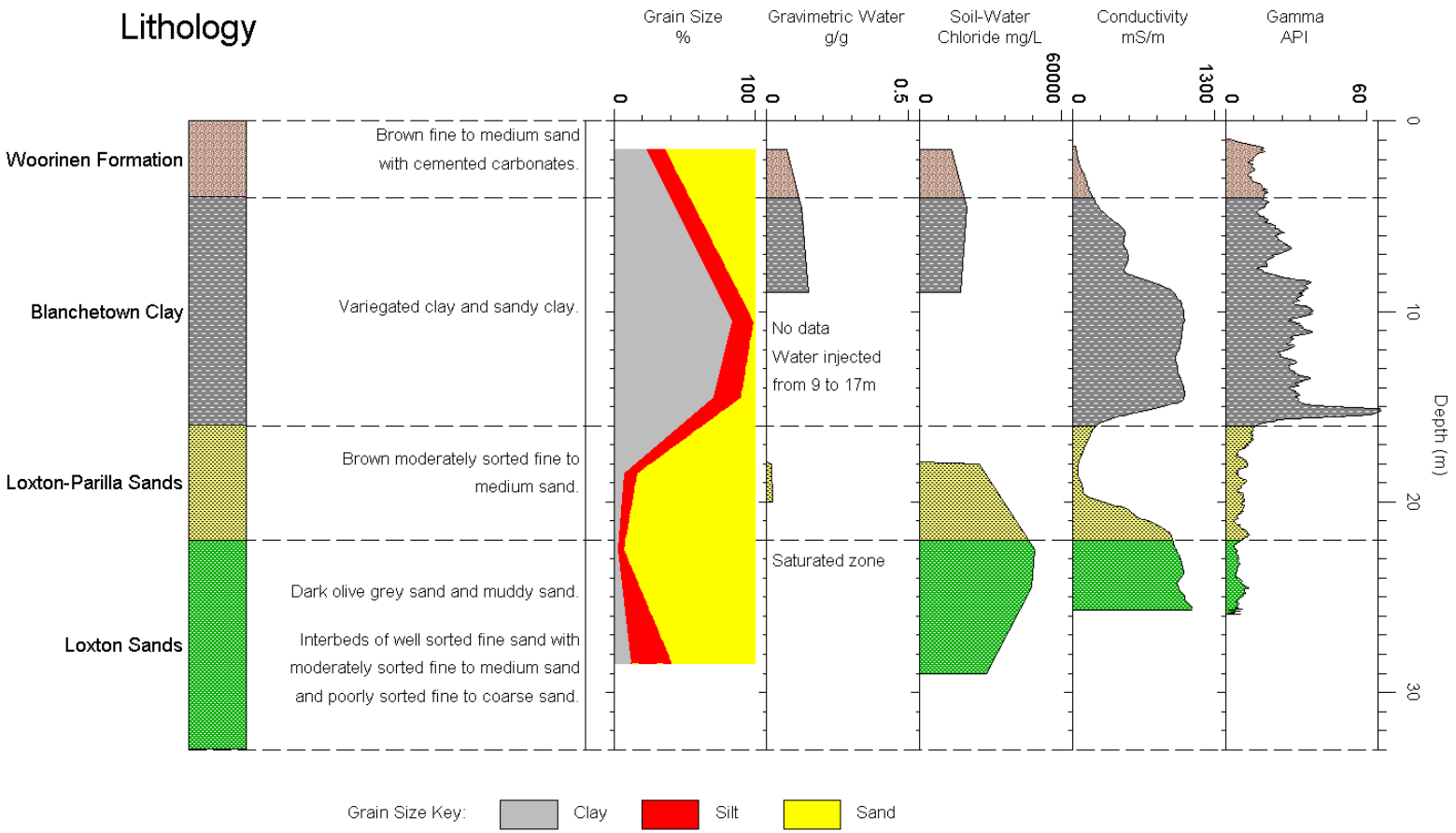
Lithology
Grain Size %
Gravimetric Water g/g
Soil-Water Chloride mg/L
Conductivity mS/m
Gamma API
0
100
0
0.5
0
60000
0
1300
0
60
Woorinen Formation
Brown fine to medium sand with cemented carbonates.
Blanchetown Clay
Variegated clay and sandy clay.
No data
Water injected from 9 to 17m
Loxton-Parilla Sands
Brown moderately sorted fine to medium sand.
Saturated zone
Loxton Sands
Dark olive grey sand and muddy sand.
Interbeds of well sorted fine sand with moderately sorted fine to medium sand and poorly sorted fine to coarse sand.
Depth (m)
0
10
20
30
Grain Size Key:
Clay
Silt
Sand

Bore RIV9LC

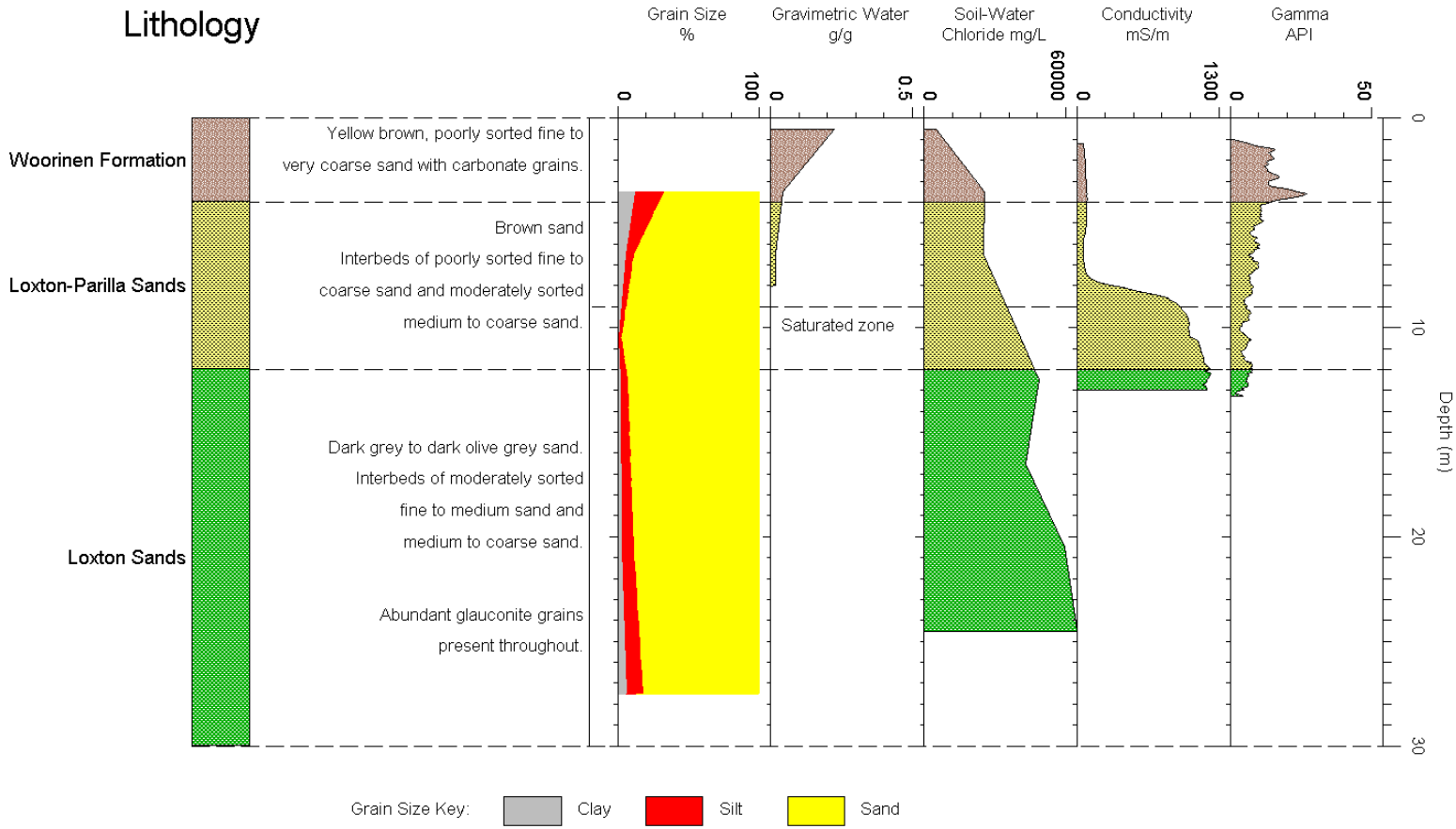
Lithology
Grain Size
%
Gravimetric Water
g/g
Soil-Water
Chloride mg/L
Conductivity
mS/m
Gamma
API
0
100
0
0.5
0
60000
0
1300
0
50
Woorinen Formation
Yellow brown, poorly sorted fine to
very coarse sand with carbonate grains.
Loxton-Parilla Sands
Brown sand
Interbeds of poorly sorted fine to
coarse sand and moderately sorted
medium to coarse sand.
Saturated zone
Loxton Sands
Dark grey to dark olive grey sand.
Interbeds of moderately sorted
fine to medium sand and
medium to coarse sand.
Abundant glauconite grains
present throughout.
Depth (m)
0
10
20
30
Grain Size Key:
Clay
Silt
Sand

6. FACTORS DETERMINING THE OBSERVED ELECTRICAL CONDUCTIVITY

This section examines the relationship between the observed apparent electrical conductivity (from downhole induction conductivity logs) and water content, salinity and particle size (texture). The intent is to establish the physical basis for using electrical conductivity to map the Blanchetown Clay and to determine whether factors other than clay materials can significantly affect an observed electrical response as might be measured by an airborne EM system.

6.1 Physical and chemical characteristics of sediments and soils in the Riverland region

6.1.1 *Water Content*

The gravimetric water content for the majority of samples collected from drill core (n = 112) fall below 10 wt. % (i.e. 0.1 g/g), with only a number of samples having high water content (e.g. 30 – 45 wt. %) (Figure 18a). The data are grouped into the six lithologic units (Figure 18b), with the Loxton-Parilla Sands having the lowest median (4 wt. %), followed by the Woorinen Formation and the Murray Group Limestone (medians of 7 wt. %). In contrast, the dolomitic sedimentary unit has the highest median (30.5 wt. %), with the Blanchetown Clay being the second highest (12 wt. %).

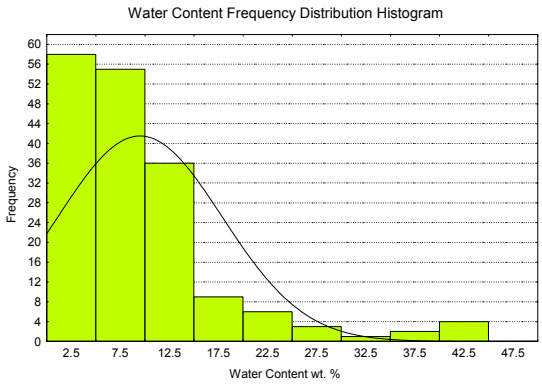

Figure 18a.
Water content distribution of all unsaturated samples (n = 174).

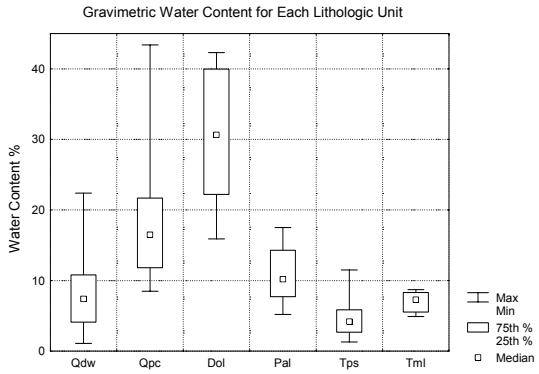

Figure 18b.
The distribution of water content of each lithologic unit.

Legend
Qdw – Woorinen Formation
Qpc – Blanchetown Clay
Dol – Dolomite bed
Pal – Palaeosol
Tps – Loxton-Parilla Sands
Tml – Murray Group Limestone

6.1.2 *Chloride Concentration*

In the unsaturated zone, the chloride (Cl) concentration of the pore water is below 30,000 mg/l (Figure 19a). Grouping the data by lithology (Figure 19b), indicates that the pore water in the Murray Group Limestone and the Dolomite beds is characterized by high Cl concentrations (median values > 20,000 mg/l). The pore water in Blanchetown Clay and the Loxton-Parilla Sands is also characterized by high Cl concentrations (16,000 and 17,500 mg/l respectively). This contrasts with the median Cl values of the pore water in both the Woorinen Formation and palaeosol (developed on Loxton-Parilla Sands) which are both low (< 5,000 and 10,0000 mg/l respectively).

The varying Cl concentrations in each lithologic unit are interpreted as reflecting differences in recharge and drainage caused by different land use practices and differences in the hydraulic transmissivity of sediments (Cook et al., 2004). These factors combine to influence the movement of salt down through the profile and the heterogeneity of Cl concentrations in the pore water.

Of the 4 bores (RIV7HC & LC; RIV9HC & LC) that intersect the groundwater, the highest chloride value is observed for saturated materials from bore RIV9LC. Values reach 65,000 mg/l. Both bores RIV9HC and LC sample the more saline groundwater of the regional system in the vicinity of the Noora evaporation basin (Figure 28). Groundwater EC reaches ~10,000 mS/m in this area. (Marsden, 2002).

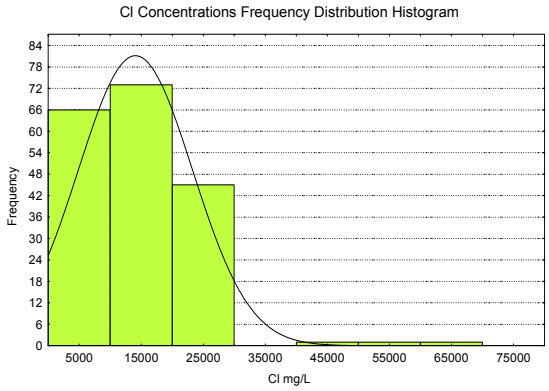

Figure 19a.
The chloride concentrations in the survey area are dominantly less than 30,000 mg/l. The highest Cl concentration is 65,000 mg/l in the saturated zone associated with highly saline groundwater close to the vicinity of the Noora evaporation basins.

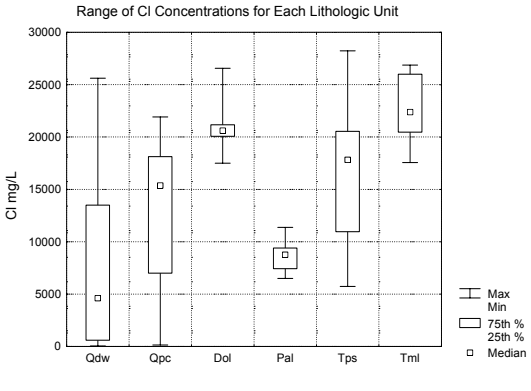

Figure 19b.
The chloride concentrations of each lithologic unit. For consistency, data from saturated samples have not been included.

Legend

Qdw – Woorinen Formation
Qpc – Blanchetown Clay
Dol – Dolomite bed
Pal – Palaeosol
Tps – Loxton-Parilla Sands
Tml – Murray Group Limestone

6.1.3 *Grain Size Distribution, Clay Abundance and Mineralogy*

The grain size distribution of most samples from drill cuttings excluding the fine-grained carbonates, comprise mainly of muddy sand and silty sand (Figure 20a). The textures of the Blanchetown Clay and a palaeosol consist of muddy sand, sandy mud, sandy clay and clay. If we consider the relative abundance of the clay fraction (< 4 µm) for samples representative of each of the main lithologic units, materials from the dolomite bed have the highest median and maximum values (Figure 20b). However, this fraction consists primarily of fine grained carbonates rather than phyllosilicates. The median values for both the Blanchetown Clay and the palaeosol (developed in the Loxton-Parilla Sands) have elevated levels of clay as compared with materials from the Woorinen Formation and the Loxton-Parilla Sands. Several samples from the Woorinen Formation that have higher clay abundance values also contain carbonate (massive calcite and dolomite) (refer to mineralogy table – Appendix B2). In this case, the clay fraction is taken to include both phyllosilicates and carbonates.

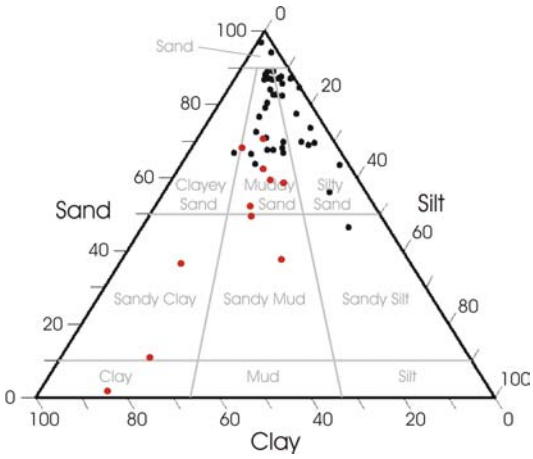

Figure 20a.
Ternary diagram of sand, silt and clay volume % using the sedimentary classification system (Lewis & McConchie, 1994). Samples obtained from Palaeosol and Blanchetown Clay are denoted by red dots.

NB: Data from Dolomite Bed and Limestone not included.

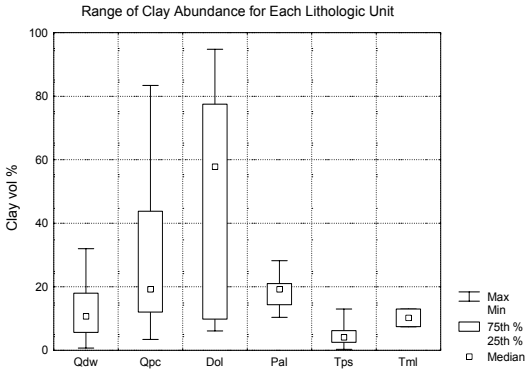

Figure 20b.
Box plot shows the range of clay abundance in each lithologic unit.

Legend:

Qdw – Woorinen Formation
Qpc – Blanchetown Clay
Dol – Dolomite bed
Pal – Palaeosol
Tps – Loxton-Parilla Sands
Tml – Murray Group Limestone

6.1.4 *Electrical Conductivity*

Grouping the electrical conductivity data, from downhole induction logs, into the six lithologic units, reveals that the Dolomite beds have the highest ECa median values (850 mS/m) (Figure 21). The Blanchetown Clay also exhibits high ECa, but the majority of measured values fall in the range 180 – 450 mS/m for the 25th – 75th percentiles respectively. The borehole inductive logs suggest that the Blanchetown Clay can be separated from other significant lithologic units, particularly the Woorinen Sands and the Loxton-Parilla Sands, since their 75th percentiles are much lower (120 and 80 mS/m respectively). Although the dolomite bed has the highest observed electrical conductivity, it is not regionally extensive and therefore would not constitute a problem from a mapping perspective. However, it might be expected to behave in a similar manner to the Blanchetown Clay in terms of its hydraulic properties. As such it could be bracketed with the clay as a desirable target for mapping using an EM system.

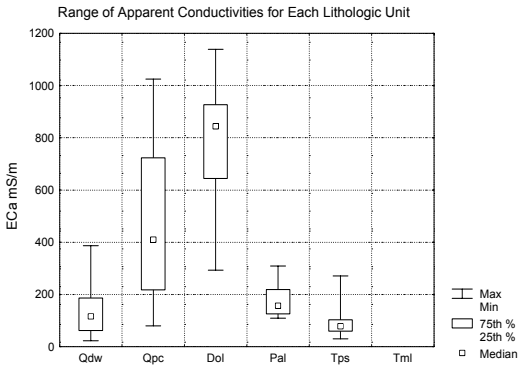

Figure 21.
Box and whiskers plot shows the range of apparent conductivity for each lithologic unit. Dolomite beds show the highest ECa, followed by Blanchetown Clay.

Legend
Qdw – Woorinen Formation
Qpc – Blanchetown Clay
Dol – Dolomite bed
Pal – Palaeosol
Tps – Loxton-Parilla Sands
Tml – Murray Group Limestone

6.2 Relationships between observed electrical conductivity and material characteristics

Rhoades et al. (1976) demonstrated that the apparent conductivity of a material is the weighted summation of the electrical conductivity of liquid and solid phases (Equation 1). In the absence of massive sulphides, conductivity is attributed to the liquid phase, which is in turn driven by the volumetric water content and the electrolyte (mainly sodium and chloride) ion concentration in the pore water.

$$ECa = ECw\theta\tau + ECs \qquad \text{Equation 1}$$

ECa is the apparent conductivity, ECw is the pore water conductivity, θ is the volumetric water content, τ is the tortuosity and ECs is the solid phase conductivity.

To avoid ambiguity in determining the principal factors driving electrical conductivity for materials collected in Riverland, carbonates samples were not included in the analyses that follow. The term 'clay' is strictly used to describe the less than 4 µm fractions that comprise phyllosilicate minerals only.

A plot of water content against clay abundance (Figure 22a) with the data points grouped according to electrical conductivity values reveals the following. The water content is positively

correlated with clay abundance. From a study of grain size distribution as described in section 6.1.3 above, sediments with a low clay content, are predominantly muddy sands and silty sands. In these materials, the water content tends to be lower than clay-rich samples (Figure 22a), which also have high electrical conductivities (Figure 22d). At saturation, the water content is determined by the porosity, which increases with increasing clay abundance (Brady, 1990). However, in the unsaturated zone, the water content varies, and depends on several factors, including the rate of recharge, evapotranspiration and soil / sedimentary textures. The first two factors are associated with precipitation and land use patterns. Prior to land clearing, the deep rooted native mallee has been effective at retrieving soil moisture, resulting in low water content in the soil. Deep drainage, *i.e.* water passes through the root zone, has been kept to a minimal (~0.1 mm/yr) (Leaney, 2000). Since clearing of the native vegetation however, recharge is noted to increase (10 mm/yr). This new recharge rate created a "wetting front", which has descended 4 m vertically since (Cook *et. al,* 2004). In other words, sediment in the wetting front will contain more moisture than sediments below the wetting front, which still reflect the hydrologic condition prior to land clearing. This may in part explain the spread of water contents contain in materials with same texture, or clay abundance. Variation in hydrologic conditions at different depths and geographic locations would account for the difference in water contents in samples with similar texture.

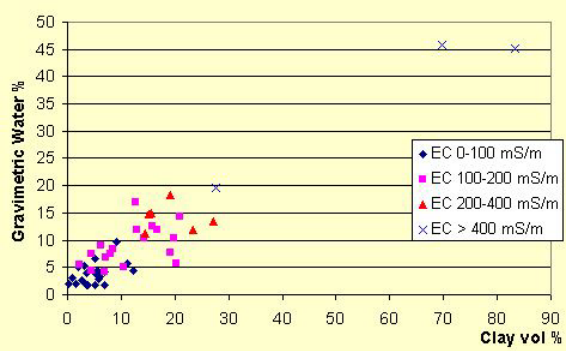

Figure 22a.
A plot of gravimetric water content against clay abundance (vol %).

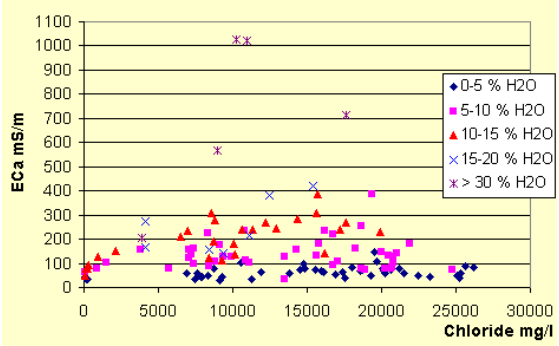

Figure 22b.
A plot of electrical conductivity against chloride concentration.

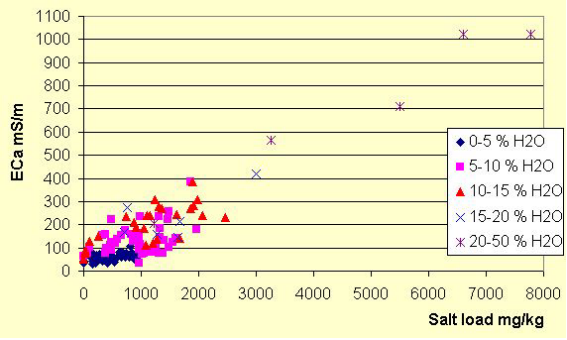

Figure 22c.
A plot of electrical conductivity against salt load (*i.e.* amount of saline pore water in a given mass of sediments.)

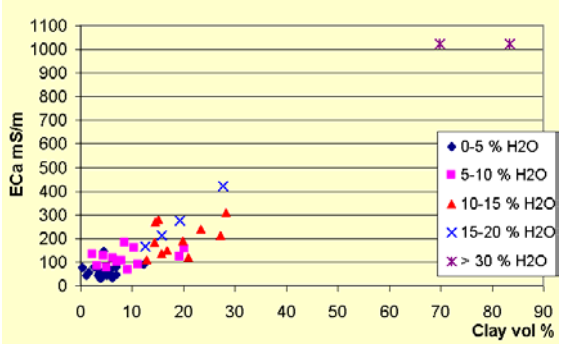

Figure 22d.
A plot of electrical conductivity against clay abundance.

The graph of electrical conductivity against chloride concentrations in the pore water shows no clear relationship (Figure 22b). Grouping the data with respect to water content however unveils a few significant trends. Except for a few samples with low saline pore water (< 2,000 mg/l), the rest of the pore waters are brackish to saline, with a wide range of chloride concentrations (up to 27,000 mg/l). Samples with moderate amounts of water (5-15 wt. %) and relatively low chloride content (<2000 mg/l) exhibit low conductivities (less than or ~ 100 mS/m). In contrast, samples with low water content (up to 5 wt. %), albeit having high chloride concentrations (> 10,000 mg/l Cl), also have low electrical conductivity (mostly < 100 mS/m). This suggests that the principal factor driving the electrical conductivity is not the salinity of the pore water alone. The two samples with highest observed electrical conductivity have a high water content (> 30 wt. %) and high chloride concentrations (approximately 10,000 mg/l). This indicates that it is the combination of the chloride content and the amount of water present that drives the apparent electrical conductivity.

The amount (mass) of saline pore water in a given unit (mass) of sediments is termed salt load. Total salt loads can be calculated by multiplying the sample water content with the sum of major cations and anions concentration. A plot of electrical conductivity against salt load (mg/kg chloride) shows a good correlation between the two ($r^2 = 0.83$) (Figure 22c). Equation 1, would suggest that an increase in salt load would lead to an increase in the electrical conductivity of the liquid phase and a rise in the overall apparent electrical conductivity (ECa). In the unsaturated zone, higher salt loads are associated with samples with high water content and clay abundance. Thus clay abundance is positively associated with the electrical conductivity (Figure 22d).

These results confirm that the remote measurement of electrical conductivity would assist in the mapping near surface clays in sediments found in the Riverland region.

6.3 Interpretation of Conductivity Patterns Identified in the RESOLVE Apparent Conductivity Images against available Borehole Data

In this section we examine RESOLVE HEM data to further validate the technology for mapping clay materials. Borehole information, as described in the previous sections, is used in this validation process. Initially we examine the apparent conductivity derived from the HEM data and cross reference the results against Conductivity Depth Images (CDI) and the map of clay thickness, which was derived from constrained inversion of the AEM data. The aim was to elucidate the value in going to a fully constrained inversion of the HEM data as distinct from the approximate CDI or apparent conductivity inversions. The areas being examined in details are shown in Figure 23 and Figures 24 a-f.

Bore RIV2HC targets high conductivity whereas RIV2LC was intended to target areas of low conductivity (< 100 mS/m) as defined in the high frequency (100 kHz and 25 kHz) apparent conductivity HEM images. These images will reflect conductivity variations in the near surface (the target zone) compared with the lower frequencies. The down-hole inductive conductivity log for RIV2LC shows only a slight decrease in ECa in bore compared to RIV2HC. This is consistent with the observed conductivity defined in the 25 kHz image (Figure 24a). The borehole information suggests that the observed apparent conductivity signature in the vicinity of these boreholes is likely to match the response from the clayey sand unit, which in this case is an interpreted palaeosol develops in the Pliocene Loxton-Parilla Sands (Figure 24a). The underlying sands and silty sands in the vicinity of these two bores are low in conductivity, and are unlikely to contribute to the elevated conductivity observed in the 25,000 Hz image.

Bores RIV3-1HC and RIV3PHC each target a patch of high conductivity ground as seen in Figure 24b. Borehole RIV3LC aims to verify the cause for a low conductivity area found in between. Borehole geological and geophysical logs suggest that the high conductivity is associated with a mud-rich Blanchetown Clay (Bore RIV3-1HC) and dolomite bed (Bores RIV3-1HC and RIV3PHC). In contrast, neither the mud-rich Blanchetown Clay nor the Dolomite Bed is present in borehole RIV3LC. In this instance, the low conductivity is associated with the Pliocene sand.

Bore RIV4LC is located in a conspicuous patch of resistive ground. In contrast, bore RIV4HC targets a conductive area (Figure 24c). In the former, borehole data indicates the presence of a poorly conducting (100-150 mS/m) Woorinen Formation overlying Loxton-Parilla Sands The presence of 2.5 m of conductive Blanchetown Clay in RIV4HC explains the observed conductivity pattern seen in the 25 kHz apparent conductivity image (Figure 24c).

In Figure 24d, the linearly orientated zone of high conductivity in the vicinity of RIV5HC is attributed to the presence of conductive fine-textured sediments, which include dolomite and sandy silt of the Pleistocene Bungunnia Limestone and Blanchetown Clay respectively. The poorly conducting surrounding areas, which were targeted with bore RIV5LC, are associated with an absence of clay and carbonate in the near surface. In bore RIV5LC only the poorly conducting sands of the Woorinen Formation and Loxton-Parilla Sands (mostly < 100 mS/m) were intersected.

Although bore RIV6HC targeted a linear conductive pattern, it was located on the western edge of the conductive area shown in the image (Figure 24e). In contrast to other bores, the conductivity is attributed to the presence of a muddy sand associated with the Blanchetown Clay and a fine to medium sand of the Loxton-Parilla Sands. The conductive response from the sands is attributed to their moderate water content (10 wt. %) and high Cl concentrations (up to 20,000 mg/l).

In the vicinity of bores RIV7LC and RIV7HC, the 25 kHz apparent conductivity image shows a narrow band of moderate to high conductors (yellows and reds) with sporadic distribution (Figure 24f). Bore RIV7HC targets one of the moderate conductors (~ 200 mS/m). Borehole information confirms the presence of a shallow conductor associated with sandy mud of the Pleistocene Blanchetown Clay. The underlying Pliocene sand has a low apparent conductivity (~50 mS/m). Bore RIV7LC was drilled in an adjacent area characterized by a low apparent conductivity as mapped in the image (Figure 24f). Although 2 m of muddy sand is present, and is interpreted to be Blanchetown Clay, the moderate conductivity (100 mS/m), combined with the underlying, poorly conductive (< 50 mS/m) Pliocene sand, results in a relatively low observed response in the HEM image (green-blue, Figure 24f).

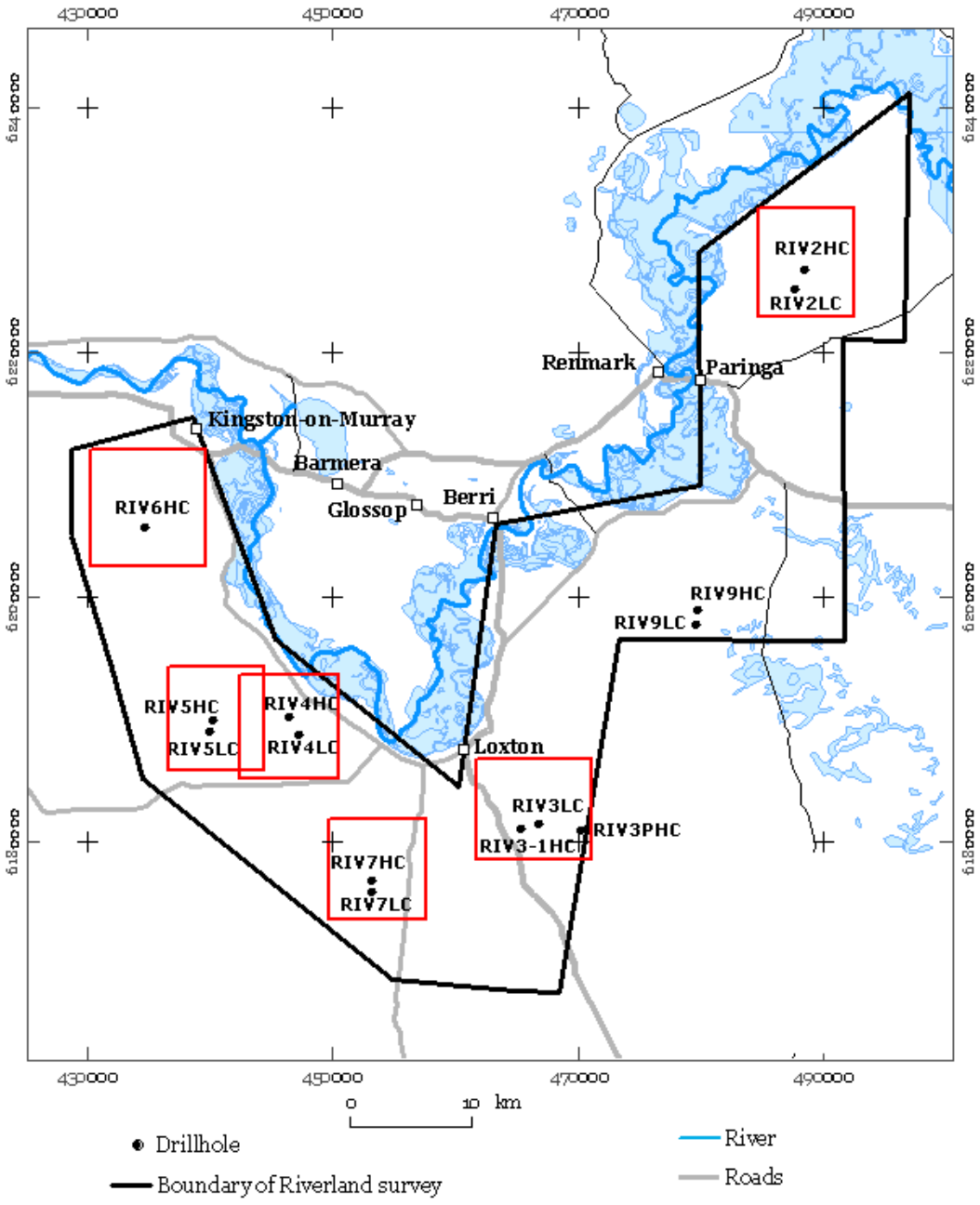

Figure 23. Bore locations in the Riverland HEM survey area. Areas enclosed by the red rectangles are shown in more details in Figures 24a-f.

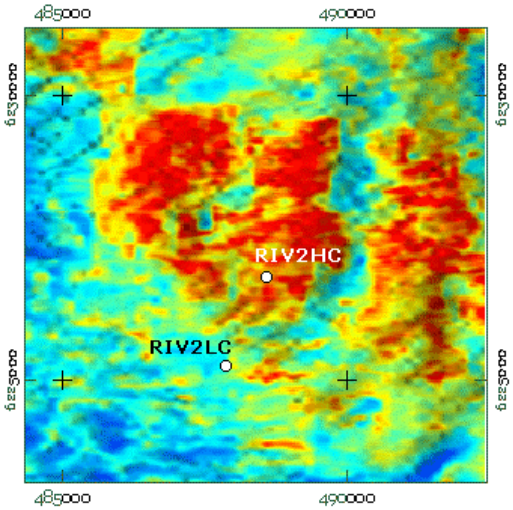

Figure 24a

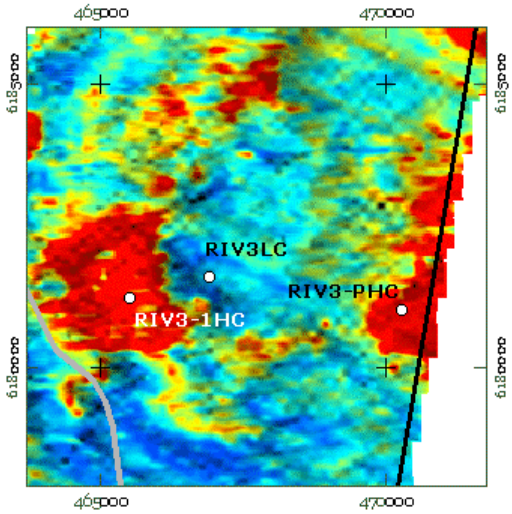

Figure 24b

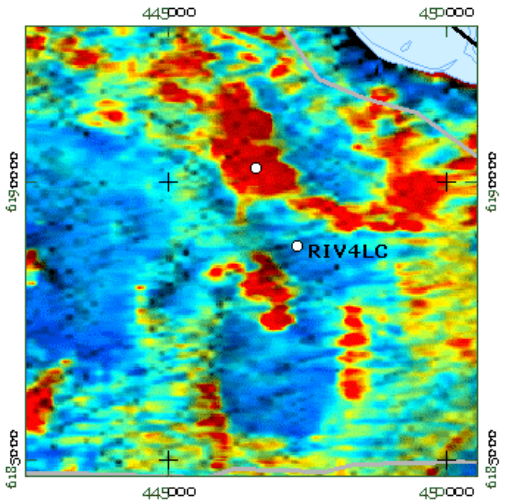

Figure 24c

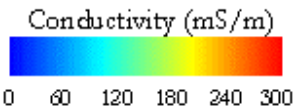

Figures 24a – c.
Closed-up view of the boreholes and the conductivity signatures shown on the 25 kHz apparent conductivity image**.**

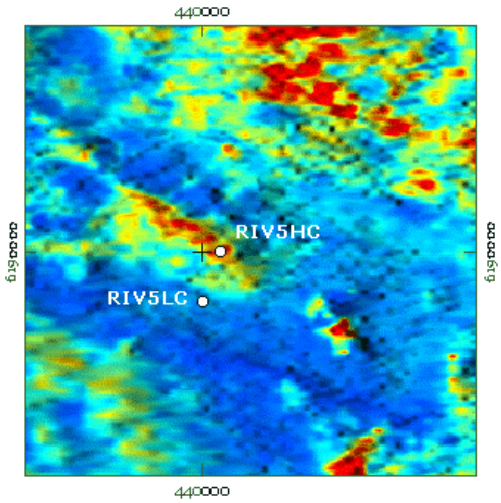

Figure 24d

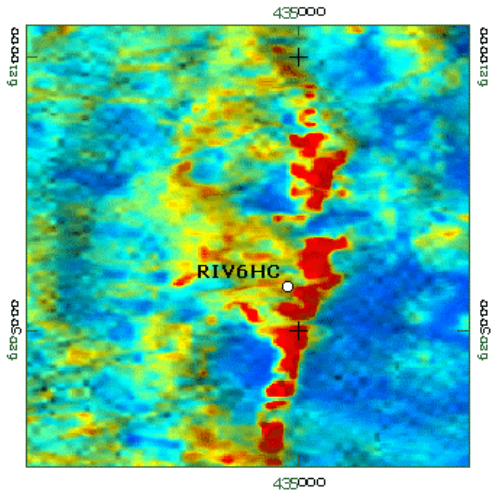

Figure 24e

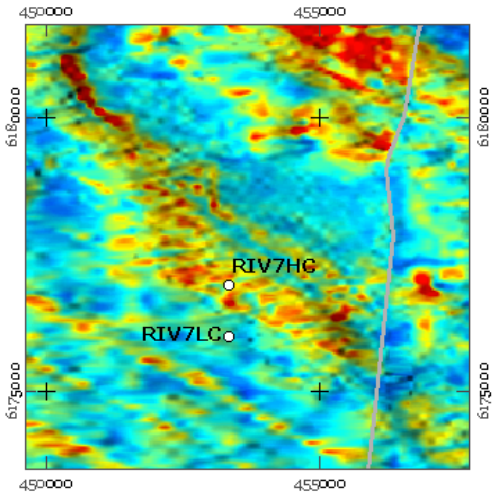

Figure 24f

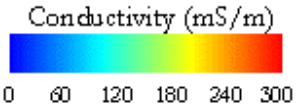

Figures 24d – f.
Closed-up view of the boreholes and the conductivity signatures shown on the 25 kHz apparent conductivity image.

6.4. Validation of the HEM Constrained Inversion Product – the Clay Thickness Image

The Resolve HEM data were inverted using a 1D layered earth inversion, constrained using prior knowledge of the depth to the watertable, and information on the average conductivities of various sedimentary units present in the study area (Green *et. al,* 2004; and Brodie *et. al,* 2004). The thickness of the 2nd layer (of a five layer model) from this inversion was intended to reflect the spatial distribution and thickness of clay in the near surface in the Riverland region (Figure 25).

The pair of boreholes RIV9HC and RIV9LC, drilled at a later date when the constrained inversion product (clay thickness image) became available, targeted an area with thick clay and an area interpreted to have no clay present in the near surface. This interpretation was confirmed by mineralogical and textural analyses of borehole cuttings and borehole conductivity logs. Results from a study of these bores, the 25 kHz apparent conductivity image and the constrained inversion product "clay thickness" confirmed the value of a full inversion of the helicopter EM data for mapping a near surface clay layer. The 25 kHz apparent conductivity image (Figure 26a) indicates that both boreholes are located in high conductivity areas, and, under normal circumstances, would suggest the presence of clay in both locations. The available borehole information confirmed the presence of thick (12 m) and conductive clay (>1,000 mS/m) in RIV9HC and the presence of shallow resistive sand in RIV9LC. The contrast is apparent in the map of clay thickness (Figure 26b) but, as mentioned above, not so in the apparent conductivity image.

Evidence from bore RIV9LC suggests that the proximity of a highly saline groundwater (50,000 mg/l Cl) near to the surface (~9m depth) results in an ambiguous response being depicted in the 25 kHz image (Figure 26a). Cross referencing with the regional groundwater contours shows that groundwater elevation in the vicinity of RIV9LC is approximately 16 m AHD (Figure 27). The surface elevation is 26 m AHD and the saturated zone (groundwater) is present at ~9 m depth, or 17 m AHD. In addition, the electrical conductivity (EC) of the groundwater is the highest EC (> 60,000 μS/cm) in the vicinity of boreholes RIV9HC and RIV9LC (Figure 28). Thus, the observed response in the apparent conductivity image appears to be related to the highly saline near surface water table. A CDI cross section (Figure 29) also shows the presence of shallow conductive groundwater (RIV9LC) and the conductive clay identified in the bore RIV9HC. These results confirm the value of adopting a full inversion approach, not least because it removes the ambiguities that otherwise be present in the areas such as found around these bores.

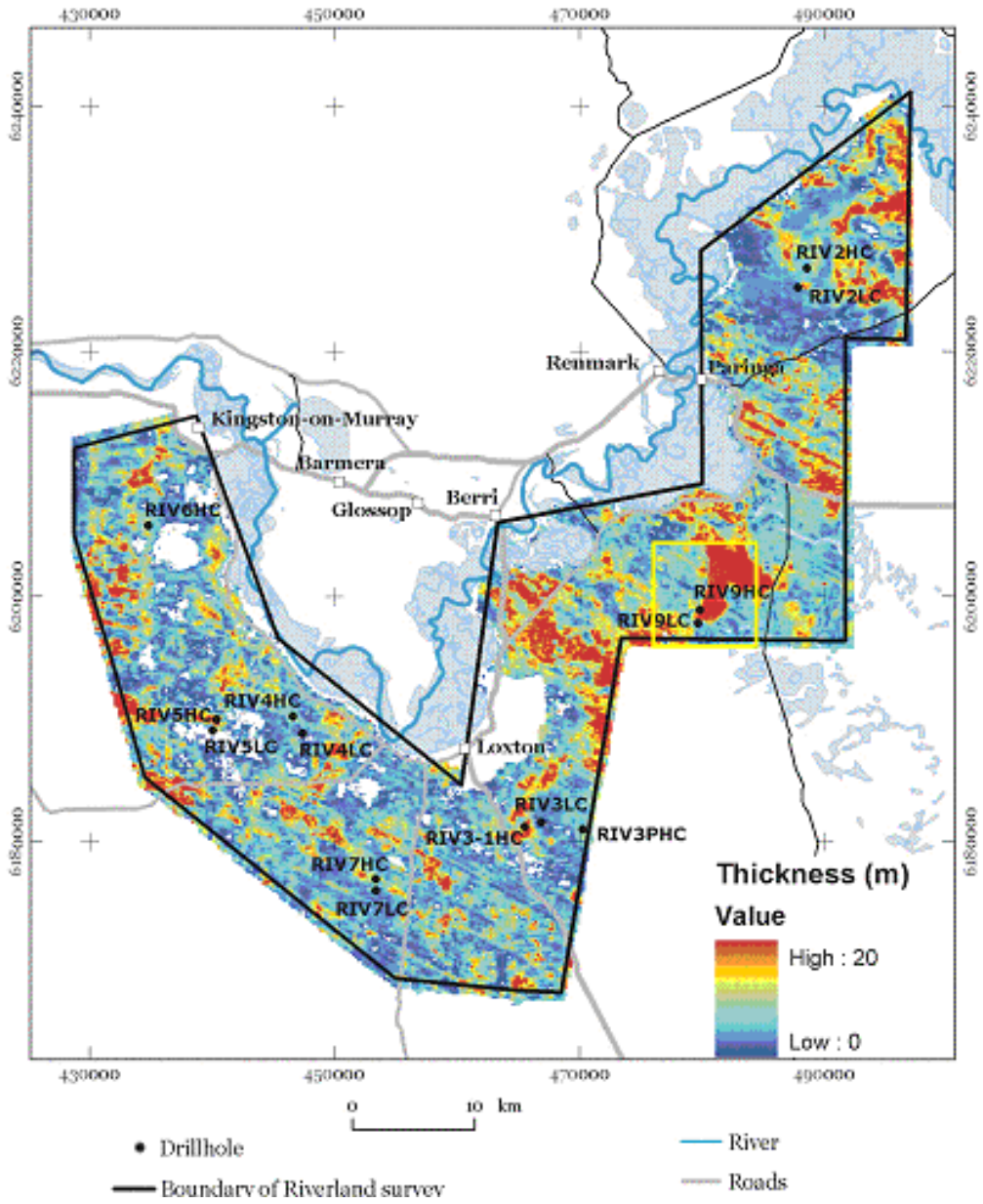

Figure 25. Pseudocoloured image of Layer 2 from the constrained inversion of the RESOLVE data for Riverland. The image reflects the spatial distribution and thickness of conductive clay (see Brodie *et. al*, 2004). The close-up view within the yellow rectangle is shown in Figures 26a & b.

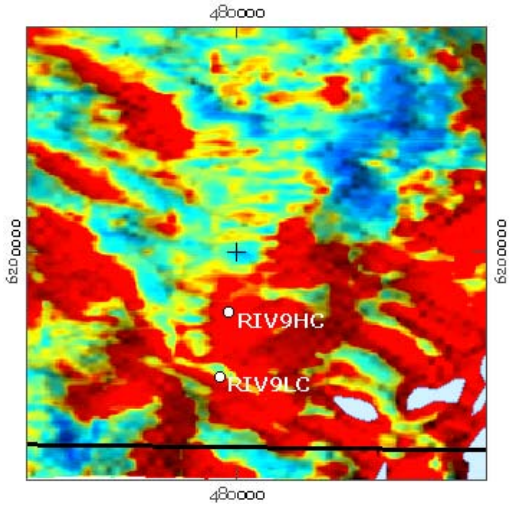

Figure 26a.
Apparent conductivity image 25 kHz shows ambiguity in conductive areas which could be associated with shallow saline groundwater, rather than clay.

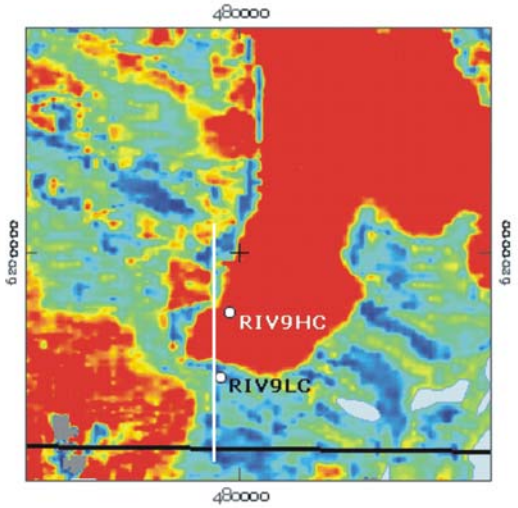

Figure 26b.
The constrained inversion product of the 2nd layer shows areas of thick clay in red. 10 m of clay is present in bore RIV9HC whereas no clay is present in RIV9LC.

There is a positive correlation between the predicted clay thickness from the constrained inversion and thickness of clay inferred from logs of pre-existing bores (Figure 30). Whilst a wide spread of data points is apparent, the general discrepancy is +/- 5 m, can be attributed to several factors, including as the heterogeneity in the clay distribution at the local scale, variations in clay thickness over the distance between a bore and the nearest flight line (Green *et al.* 2004), and possibly because of the difficulty in geologically logging the Blanchetown Clay. In places is appears more like a sand than a clay and depending on the drilling approach may have been logged as such. In some instances, the thickness of clay has been grossly over-predicted, possibly caused by a breakdown in the 1-D assumption used in the inversion. In other instances, the thickness of clay has been grossly under-estimated. This may result from errors in the geological logging and/or the presence of sandy mud that contains either non saline pore fluid, or low water content, with associated low conductivity.

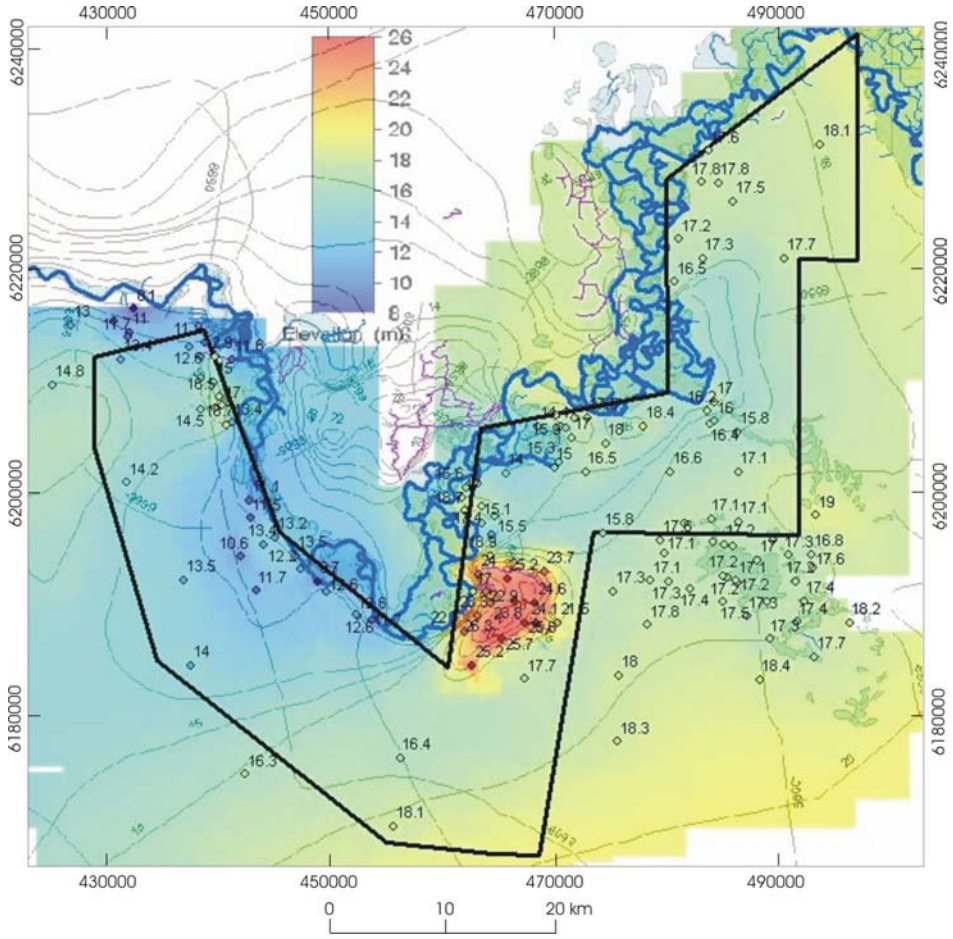

Figure 27. The Groundwater level contours show a gentle gradient towards the river. A groundwater mound is present underlying the Loxton irrigation area. **(**Source: Data provided by S. Barnett, image created by R. Brodie)

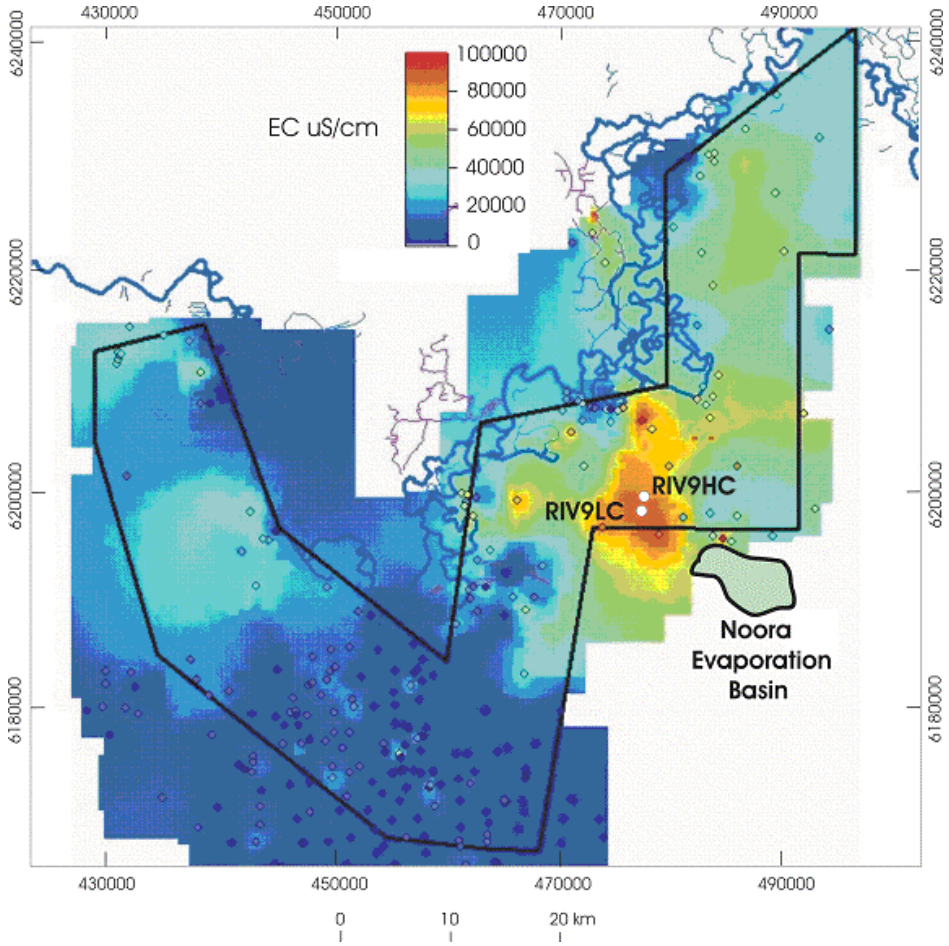

Figure 28. Groundwater electrical conductivity image showing high EC towards the east of the survey area in close proximity to the Noora Evaporation Basin.(Source: Data provided by S. Barnett, image created by R. Brodie)

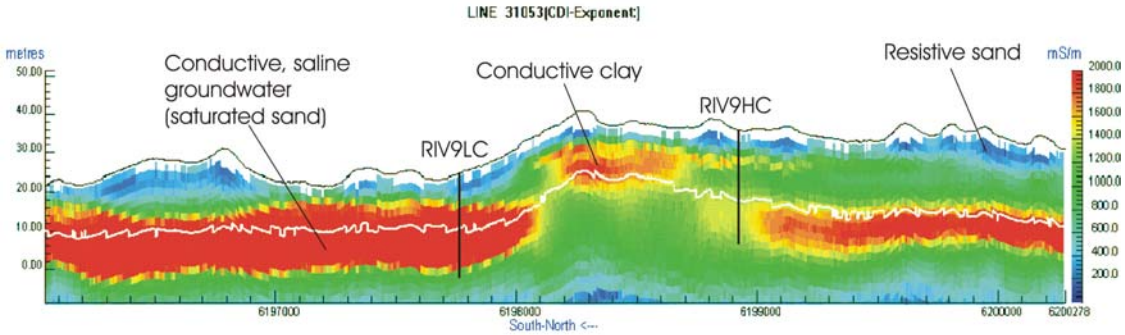

Figure 29. CDI cross section shows the presence of shallow conductive groundwater (saturated sand, RIV9LC) and the presence of shallow conductive clay (RIV9HC) **(**Source: Andrew Fitzpatrick).

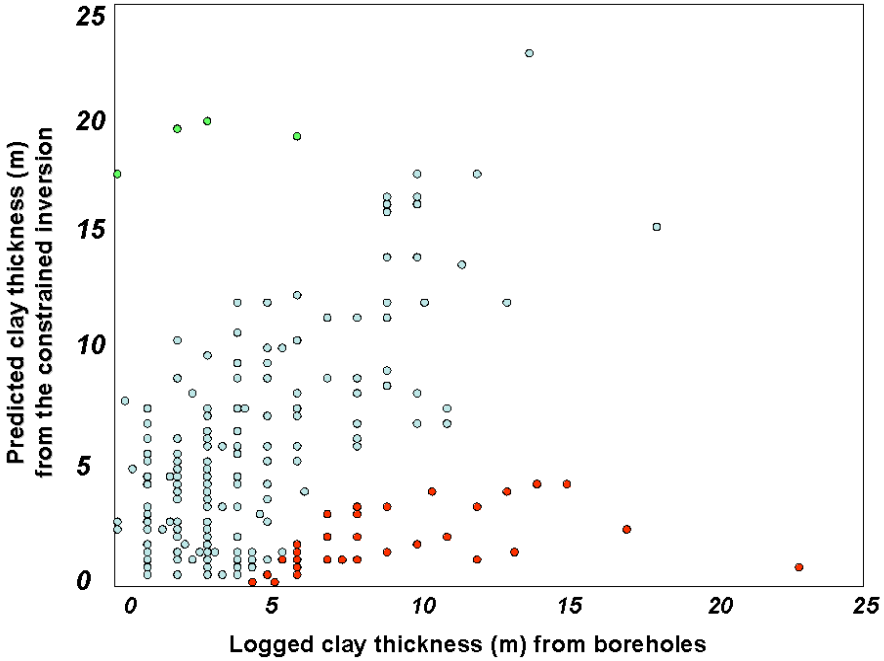

Figure 30. Scatter plot of clay thickness predicted from constrained inversion of AEM data and thickness from lithological logs. Accepting errors that could arise in the visual logging (eg the red data points), there is reasonable correlation. Other outliers may be attributed to noise in the AEM data and/or a breakdown of the 1-D assumption used in the inversion (source: Green *et al.,* 2004).

7. CONCLUSION

The Following a comprehensive study to ground validate the airborne electromagnetic data, the following can be concluded.

In the Riverland AEM survey area, variations in the observed electrical conductivity (ECa) of near surface materials are primarily determined by the texture of sediments. A detailed analysis of texture and water content established that finer textured materials are generally characterized by higher water contents. Although chloride concentrations may vary, and remain high in sand-rich materials, the low water content associated with sand and the higher water content associated with clay-rich sediments resulted in a low ECa for the former and an elevated ECa for the latter.

Textural information and borehole conductivity logs obtained from the 14 selected boreholes, which target specific conductivity patterns shown on the high frequency (25,000 Hz) apparent conductivity image, suggest that the observed conductivity response is largely determined by the distribution of near surface clayey materials. A discrepancy arises in the vicinity of low lying areas where shallow and saline groundwater occurs, in which case, the conductivity signature is attributed to conductive saturated sand. A comparison between inversion procedures (apparent conductivity, CDI and a constrained 1D Layered Earth Inversion) in the vicinity of borehole RIV9HC and RIV9LC shows that the RESOLVE HEM system is capable of differentiating between conductive shallow clay and a saline, conductive groundwater (i.e. saturated sand). The best results from a clay mapping perspective, were obtained from the constrained inversion confirming the value of a full inversion in reducing ambiguities.

8. REFERENCES

Brady, N.C. 1990. The Nature and Properties of Soils. McMillan Publishing Company, New York: 621 pp.

Brodie, R., Green, A. and Munday, T., 2004, Constrained inversion of helicopter AEM data for mapping the Blanchetown Clay: Extended Abstracts ASEG 17th Geophysical Conference and Exhibition, Sydney 2004.

Brown, C.M. and Stephenson, A.E. 1991. Geology of the Murray Basin. Southeastern Australia. Department of Primary Industries and Energy, Bureau of Mineral Resources, Geology and Geophysics. Bulletin 235. 430 pp.

Cook, P. and Kilty, S., 1992, A helicopter-borne electromagnetic survey to delineate groundwater recharge rates: Water Resources Research, 28, 2953-2961.

Cook, P.G., Leaney, F.W. and Jolly, I.D. 2001. Groundwater recharge in the Mallee Region, and salinity implications for the Murray River – A Review. CSIRO Land and Water, Technical Report No. 45/01. 133 pp.

Cook, P.G., Leaney, F.W. and Miles, M. 2004. Groundwater Recharge in the North-East Mallee Region. CSIRO Land and Water, Technical Report No. 25/04. 80 pp.

Cowey, D., Garrie, D. and Tovey, A., 2003, Riverland and Tintinara, South Australia, RESOLVE Geophysical Survey, acquisition and processing report. Report to the Bureau of Rural Sciences, available from Geoscience Australia.

Green, A., Brodie, R. and Munday, T., 2004, Interpretation of helicopter AEM data of the Riverland Area, South Australia: Extended Abstracts ASEG 17th Geophysical Conference and Exhibition, Sydney 2004.

Jones, G. and Henschke, C. 2003. South Australia Salinity Mapping and Management Support: Jamestown drilling Report – A draft report to the technical committee: Bureau of Rural Science.

Leaney, F.W. 2000. Groundwater Salinisation in the Tintinara area of South Australia, results of field investigations, April 2000: CSIRO Land and Water, Technical report 34/00.

Leaney, F.W., Barnett, S., Davies, P., Maschmedt, D., Munday, T. and Tan, K. 2004. Groundwater Salinsation in the Tintinara Highland Area of SA: revised estimates using spatial variation for clay content in the unsaturated zone. CSIRO Land and Water, Technical report 24/04. 62 pp.

Lewis, D.W. and McConchie, D. 1994. Practical Sedimentology. Chapman and Hall, New York. 213 pp.

Marsden, Z.E. 2002. Noora Prescribed Wells Area Groundwater Monitoring Status Report 2002/08: The Department of Water, Land and Biodiversity Conservation. 18 pp.

Moore, D.M. and Reynolds, Jr. R.C. 1989. X-ray Diffraction and the Identification of Clay Minerals, Oxford University Press, Oxford.

Munday, T.J., Green, A.A., Brodie, R.C., Lane, R., Sattel, D., Barnett, S.R., Cook, P.G. and Walker, G. 2003. Developing recharge reduction strategies in the Riverland of South Australia using airborne electromagnetic data – a case study in tailoring airborne geophysics given a particular target and a desired set of outcomes. Extended abstracts, 16th ASEG 2003 Conference, Adelaide. 4pp.

Rawle, A. 2001. Basic Principles of Particle Size Analysis: Technical Paper MRK043, Malvern Instruments Limited.

Rhoades, J.D., Raats, P.A.C. and Prather, R.S. 1976. Effects of Liquid-Phase Electrical Conductivity, Water Content, and Surface Conductivity on Bulk Soil Electrical Conductivity: Soil Science Society of America Journal, 40, 651-665.

9. ACKNOWLEDGEMENTS

The Riverland AEM survey was funded by the South Australia Salinity Mapping and Management Support Project (SA-SMMSP), under the auspices of the National Action Plan. Steve Barnett (DLWBC) is thanked for providing groundwater and salinity information and additional bore hole data. Megan LeFournour (CSIRO L&W) is thanked for laboratory analysis of drill cores and cuttings. The authors expressed gratitude to John Spring (BRS) for acquiring the down-hole geophysical logs. Heike Apps and Penny Kilgour (GA) have assisted in the GIS and are much appreciated. Thanks also to the land holders and companies for allowing access to drill sites. Staff from SA Water is thanked for field logistic support. David Gibson (GA), Ross Brodie (GA/ANU), Richard Lane (GA), Andrew FitzPatrick (GA), Mathew Gray (GA), John Wilford (GA), Patricia Please (GA), Dirk Kirste (ANU), Jonathan Clarke (GA), and Andy Green (OTBC) are thanked for pertinent discussion on geomorphology, groundwater, geology and geophysics. Mary Walsh (GA) is thanked for her administrative assistance.

10. APPENDICES

10.1 APPENDIX 1 – METHODS

10.1.1 Borehole

Fourteen bores were drilled in the AEM survey area to validate the observed electrical conductivity response in the AEM data. Nine bores (RIV2HC/LC to RIV6HC) were drilled using a hollow stem auger corer. The hollow stem auger coring method allows half metre continuous cores to be collected. The sample recovery was generally good, except in sand-rich units where some material was lost. The cores were split into two halves. One half of the core was stored in glass jars and sent for gravimetric water content and soil-water Cl analyses. The other half was stored in core-trays for lithology logging, grain size and mineralogical analyses.

Four bores (RIV7HC/LC and RIV9HC/LC) were drilled using air-coring method. The air-coring technique produces drill cuttings, which were collected as every metre composite. This method has the advantage over auger coring as greater depths (e.g. 57 m) can be acquired.

10.1.2 Grain Size Distribution

Knowing the grain size distribution enables the validation of textural information, helps in interpretation of sedimentary environments, and aid establish relationships between sedimentary texture and down-hole electrical conductivity and salinity. 98 samples, each weighing approximately 20 g, were analysed for particle size using the Mastersizer™ laser diffraction instrument produced by Malvern Instruments, and the results are shown in Table 5.

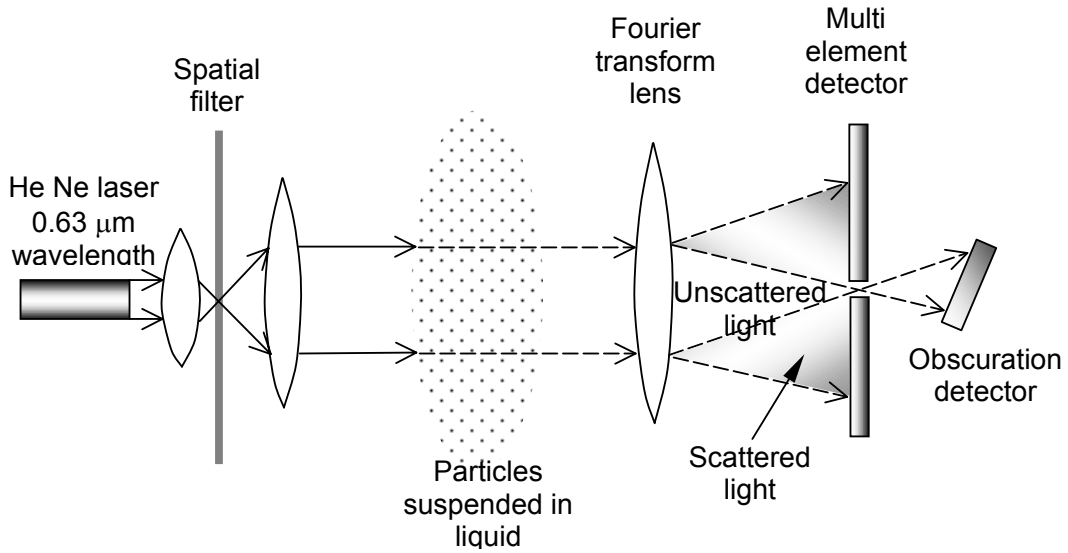

Figure 31. Schematic diagram shows the main components of a laser diffractometer. This technique allows the calculation of size fractions in volume % rather than weight %, such as those calculated using the sieving method. Source: Rawle (2001)

The laser diffraction instrument consists of three parts, a laser source (He-Ne gas or diodes emitter), detectors, and sample chamber that allows suspended particles to recirculate in front of the laser beam (Figure 31). The Mie theory (Rawle, 2001) was used to solve the equations for interaction of light with matter and calculates the volume of the particle. This technique calculates the % volume of a range of particle sizes (0.05 – 2000 μm), and the results are grouped according to the Wentworth scale. To standardise with other analytical data, SI units (μm) were reported instead of Phi units (Table 4).

Table 4. Particle size in SI units (μm), Wentworth scale.

Size Fraction	Lower boundary	Upper boundary
Very coarse sand	1000	2000
Coarse sand	500	1000
Medium sand	250	500
Fine sand	125	250
Very fine sand	62.5	125
Coarse silt	31	62.5
Medium silt	15.6	31
Fine silt	7.8	15.6
Very fine silt	4	7.8
Clay	0.06	4

10.1.3 Mineral Composition

47 samples were analysed for mineral composition, using the X-ray diffraction (XRD) technique. Individual samples were homogenised before approximately 5 g was removed and ground in a mortar with a pestle with the addition of ethanol to a fine, talc-like consistency (1-10 μm), so as to optimise diffraction (Moore and Reynolds, 1989). Each finely crushed sample was dried and randomly packed into a U-shaped aluminium holder covered with frosted glass slide (to overcome preferred orientation of crystallites). The glass slide was then removed and most samples were analysed using a Siemens™ D5000 series X-ray diffractometer (Co-Kα), and scanned from 4 ^{o} to 80 ^{o} 2θ, at a speed of 2 ^{o} per minute, and a step size of 0.02 ^{o}. The remainder were analysed using a Siemens™ D501 (Cu-Kα), and scanned from 2 ^{o} to 70 ^{o} 2θ with the same settings as above.

Mineral identification software EVA™ was used to identify the d-spacings of a series of peaks corresponding to individual minerals, and the results are shown in Table 6.

10.1.4 Down-hole Electrical Conductivity Log

The down-hole conductivity logs were carried out by John Spring from BRS using a down hole induction logging tool (Auslog-Scintrex A34). Conductivity is measured in milli-Siemens per metre (mS/m) and the instrument was calibrated using calibration rings of 100, 300 and 1000 mS/m prior to logging. A polynomial function was utilised by the software AUSWIN to transform the calibrated values. Two sets of logs were recorded as the probe was lowered, then retrieved, at a speed of 5 m per minute and values were recorded every 0.05 m (5 cm) interval.

The best set of log (with no/least anomalous artefacts) was then utilised for interpretation (Jones and Henschke, 2003).

10.1.5 Down-hole Gamma Log

The down-hole gamma logs were carried out by John Spring from BRS using Auslog-Scintrex A75 gamma tool. The natural gamma radiation was recorded in three-bands (ie. K, U, Th) as counts per seconds and subsequently converted to the standard units API (American Petroleum Institute) using the software AUSWIN. Same as the down-hole conductivity logs, two sets of logs were recorded as the probe was lowered, then retrieved, at a speed of 5 m per minute and values were recorded every 0.05 m (5 cm) interval. The best set of log (with no/least anomalous artefacts) was then utilised for interpretation (Jones and Henschke, 2003).

10.2. APPENDIX 2 – ANALYTICAL RESULTS

Table 5. Grain Size Distribution

		Size Fractions (microns) and % Volume						
		Clay	Silt	Fine Sand	Med.Sand	C / VC Sand	Granule	Interpreted
Drill hole	Depth m	<4	4 - 62.5	62.5 - 250	250 - 500	500 - 2000	>2000	Unit
RIV2HC	0.7	1.1	28.5	49.4	17.1	3.8		*Woorinen Fm*
RIV2HC	1.4	32.0	20.4	25.1	18.1	4.5		*Woorinen Fm*
RIV2HC	3.3	28.2	22.4	24.5	20.3	4.6		*palaeosol*
RIV2HC	4.7	15.2	14.4	32.1	31.5	6.8		*palaeosol*
RIV2HC	6.3	19.8	13.8	33.6	28.3	4.6		*palaeosol*
RIV2HC	8.3	10.4	10.6	36.8	35.4	6.8		*palaeosol*
RIV2HC	9.6	27.2	20.8	25.9	20.6	5.5		*palaeosol*
RIV2HC	11.3	19.2	18.7	26.5	26.8	8.8		*palaeosol*
RIV2HC	13.3	11.2	19.3	28.8	29.7	10.9		*Loxton-Parilla Sands*
RIV2HC	14.8	2.0	34.6	37.6	21.0	4.8		*Loxton-Parilla Sands*
RIV2LC	0.3	4.3	33.8	38.5	19.3	4.1		*Woorinen Fm*
RIV2LC	1.7	3.3	55.4	27.3	10.2	3.8		*Woorinen Fm*
RIV2LC	2.7	14.5	18.1	36.9	25.0	5.6		*Woorinen Fm*
RIV2LC	5.3	14.3	15.1	33.5	29.0	8.1		*palaeosol*
RIV2LC	7.7	12.9	10.7	37.2	33.2	5.9		*palaeosol*
RIV2LC	10.7	21.0	11.0	27.3	32.2	8.6		*palaeosol*
RIV2LC	14.4	5.9	6.0	36.9	44.0	7.2		*Loxton-Parilla Sands*
RIV2LC	15.7	1.0	12.0	33.7	43.0	10.3		*Loxton-Parilla Sands*
RIV3PHC	0.3	7.6	46.9	29.6	12.3	3.6		*Woorinen Fm*
RIV3PHC	1.7	31.9	11.9	35.4	18.7	2.1		*Woorinen Fm*
RIV3PHC	3.4	23.4	10.1	45.1	20.4	1.1		*Woorinen Fm*
RIV3PHC	4.3	13.3	17.9	48.0	20.2	0.6		*Woorinen Fm*
RIV3PHC	5.3	21.9	56.5	17.5	3.9	0.0		*dolomite bed*
RIV3PHC	7.3	57.8	27.5	12.0	2.7	0.0		*dolomite bed*
RIV3PHC	10.7	77.5	19.2	3.3	0.0	0.0		*dolomite bed*
RIV3PHC	11.7	9.8	32.3	44.8	13.1	0.0		*dolomite bed*
RIV3-1HC	0.7	12.2	44.8	27.1	12.8	3.1		*Woorinen Fm*
RIV3-1HC	1.7	3.1	54.6	33.6	6.6	2.0		*Woorinen Fm*
RIV3-1HC	2.7	14.0	34.9	36.1	12.6	2.4		*Woorinen Fm*
RIV3-1HC	4.6	43.8	16.5	27.1	11.7	0.9		*Bungunnia Lst*
RIV3-1HC	5.8	30.2	18.7	38.0	13.0	0.0		*Blanchetown Clay*
RIV3-1HC	6.8	12.0	6.0	57.7	24.1	0.1		*Blanchetown Clay*
RIV3-1HC	8.8	11.7	46.6	31.8	9.8	0.0		*Blanchetown Clay*
RIV3-1HC	10.4	3.4	87.8	7.3	1.3	0.1		*Blanchetown Clay*
RIV3-1HC	11.6	94.8	5.2	0.0	0.0	0.0		*dolomite bed*

Table 5. Continued		**Size Fractions (microns) and % Volume**						
		Clay	**Silt**	**Fine Sand**	**Med.Sand**	**C / VC Sand**	**Granule**	**Interpreted**
Drill hole	**Depth m**	**<4**	**4 - 62.5**	**62.5 - 250**	**250 - 500**	**500 - 2000**	**>2000**	**Unit**
RIV3-1HC	13.4	6.1	46.7	44.8	2.4	0.0		*dolomite bed*
RIV3-1HC	15.7	70.9	23.3	5.6	0.2	0.0		*dolomite bed*
RIV3-1HC	16.7	34.4	49.4	6.9	5.9	3.4		*dolomite bed*
RIV3LC	0.8	15.7	17.0	44.2	18.4	4.7		*Woorinen Fm*
RIV3LC	2.7	8.5	45.2	31.2	15.0	0.1		*Woorinen Fm*
RIV3LC	4.7	7.0	10.1	62.1	20.7	0.1		*Loxton-Parilla Sands*
RIV3LC	8.3	0.3	15.3	15.2	12.9	5.7	50.5	*Loxton-Parilla Sands*
RIV3LC	11.3	4.5	18.2	70.0	7.3	0.0		*Loxton-Parilla Sands*
RIV3LC	12.7	2.9	27.9	54.2	6.4	8.6		*Loxton-Parilla Sands*
RIV4LC	0.3	2.8	13.5	52.4	19.6	11.7		*Woorinen Fm*
RIV4LC	1.3	15.8	11.9	43.2	23.5	5.6		*Woorinen Fm*
RIV4LC	3.3	8.0	36.1	40.3	14.9	0.7		*Woorinen Fm*
RIV4LC	6.3	5.6	7.4	81.9	5.1	0.0		*Loxton-Parilla Sands*
RIV4LC	8.3	3.2	23.3	65.6	7.9	0.0		*Loxton-Parilla Sands*
RIV4LC	11.3	6.8	10.6	53.3	5.1	7.9	16.3	*Loxton-Parilla Sands*
RIV4LC	13.7	4.5	26.2	60.4	8.9	0.0		*Loxton-Parilla Sands*
RIV4LC	15.5	11.3	9.8	76.1	2.8	0.0		*Loxton-Parilla Sands*
RIV4LC	17.5	11.7	14.3	48.0	11.0	15.0		*Murray Group Lst*
RIV5HC	0.5	0.7	25.7	50.4	17.8	5.4		*Woorinen Fm*
RIV5HC	1.6	22.4	13.9	28.0	28.7	7.0		*Woorinen Fm*
RIV5HC	3.6	7.1	23.2	27.9	35.6	6.2		*Woorinen Fm*
RIV5HC	5.2	55.4	13.6	20.1	10.2	0.7		*Bungunnia Lst*
RIV5HC	6.3	27.6	34.9	24.9	12.2	0.4		*Blanchetown Clay*
RIV5HC	8.7	11.0	50.5	28.4	10.0	0.0		*Blanchetown Clay*
RIV5HC	10.7	2.3	0.8	63.4	33.4	0.0		*Loxton-Parilla Sands*
RIV5HC	12.3	2.6	10.0	56.8	30.7	0.0		*Loxton-Parilla Sands*
RIV5LC	0.3	4.3	16.9	46.7	19.9	12.2		*Woorinen Fm*
RIV5LC	1.7	6.3	11.2	61.6	19.9	1.0		*Woorinen Fm*
RIV5LC	4.7	3.6	7.2	84.2	5.0	0.0		*Loxton-Parilla Sands*
RIV5LC	8.3	5.1	8.3	81.4	5.2	0.0		*Loxton-Parilla Sands*
RIV5LC	11.7	6.9	6.6	70.7	3.8	4.1	7.9	*Loxton-Parilla Sands*
RIV5LC	14.3	7.4	13.6	24.0	6.2	10.4	38.4	*Murray Group Lst*
RIV5LC	15.8	13.0	27.9	33.3	6.3	19.4		*Murray Group*

								Lst
Table 5. Continued		**Size Fractions (microns) and % Volume**						
		Clay	**Silt**	**Fine Sand**	**Med.Sand**	**C / VC Sand**	**Granule**	**Interpreted**
Drill hole	**Depth m**	**<4**	**4 - 62.5**	**62.5 - 250**	**250 - 500**	**500 - 2000**	**>2000**	**Unit**
RIV6HC	0.7	1.6	8.2	64.2	26.0	0.0		*Woorinen Fm*
RIV6HC	1.6	6.1	25.0	49.0	19.8	0.0		*Woorinen Fm*
RIV6HC	4.6	5.1	12.8	59.3	22.7	0.0		*Woorinen Fm*
RIV6HC	6.3	9.2	10.4	54.6	22.9	2.9		*Woorinen Fm*
RIV6HC	8.3	16.8	24.9	40.3	15.4	2.6		*Blanchetown Clay*
RIV6HC	14.8	4.4	6.0	79.1	10.5	0.0		*Loxton-Parilla Sands*
RIV6HC	15.7	13.0	29.0	54.0	4.1	0.0		*Loxton-Parilla Sands*
RIV7HC	2.5	20.2	16.1	25.8	19.9	17.9		*Woorinen Fm*
RIV7HC	4.5	37.7	19.0	28.9	13.9	0.6		*Blanchetown Clay*
RIV7HC	14.5	3.4	11.0	60.6	25.0	0.0		*Loxton-Parilla Sands*
RIV7HC	22.5	3.5	9.6	66.4	15.4	5.1		*Loxton-Parilla Sands*
RIV7HC	39.5	25.1	54.6	18.7	1.3	0.2		*Murray Group Lst*
RIV7HC	50.5	17.6	45.5	28.0	4.2	4.7		*Murray Group Lst*
RIV7LC	2.5	12.6	20.7	46.0	18.0	2.8		*Woorinen Fm*
RIV7LC	8.5	1.6	4.5	6.3	22.0	65.5		*Loxton-Parilla Sands*
RIV7LC	16.5	3.8	7.5	27.2	29.1	32.5		*Loxton-Parilla Sands*
RIV9HC	1.5	23.0	12.8	27.1	19.2	17.8		*Woorinen Fm*
RIV9HC	10.5	83.4	15.1	1.4	0.0	0.0		*Blanchetown Clay*
RIV9HC	14.5	69.8	19.7	9.5	1.0	0.0		*Blanchetown Clay*
RIV9HC	18.5	6.8	9.2	5.5	17.1	61.4		*Loxton-Parilla Sands*
RIV9HC	22.5	2.5	4.2	2.4	17.6	73.3		*Loxton-Parilla Sands*
RIV9HC	28.5	11.9	29.0	21.8	18.6	18.7		*Loxton-Parilla Sands*
RIV9LC	3.5	12.2	19.9	29.4	24.0	14.5		*Loxton-Parilla Sands*
RIV9LC	6.5	5.1	6.2	6.9	21.7	60.1		*Loxton-Parilla Sands*
RIV9LC	10.5	0.3	1.9	2.2	9.7	85.8		*Loxton-Parilla Sands*
RIV9LC	12.5	1.8	5.4	10.4	17.5	65.0		*Loxton-Parilla Sands*
RIV9LC	20.5	2.7	8.5	39.6	21.7	27.5		*Bookpurnong Beds*
RIV9LC	27.5	6.2	11.7	38.5	20.6	22.9		*Bookpurnong Beds*

Table 6. Mineral Composition

		Minerals					Interpreted
Drill Hole	Depth m	Dominant Mineral	Less Abundant		Trace		Unit
RIV2HC	1.4	Quartz	Calcite	Dolomite	Kaolinite		*Woorinen Fm*
RIV2HC	4.7	Quartz			Kaolinite		*Palaeosol*
RIV2HC	6.3	Quartz	Montmorillonite	Kaolinite	Muscovite		*Palaeosol*
RIV2HC	13.3	Quartz	Kaolinite				*Loxton-Parilla Sands*
RIV2LC	2.7	Quartz	K-feldspar	Calcite	Dolomite	Kaolinite	*Woorinen Fm*
RIV2LC	7.7	Quartz			Kaolinite	Goethite	*Palaeosol*
RIV2LC	10.7	Quartz	Montmorillonite	Kaolinite			*Palaeosol*
RIV2LC	14.4	Quartz			Kaolinite		*Loxton-Parilla Sands*
RIV3P HC	3.4	Quartz	Dolomite		Kaolinite		*Woorinen Fm*
RIV3P HC	5.3	Quartz	Kaolinite				*Dolomite Bed*
RIV3P HC	10.7	Dolomite	Quartz				*Dolomite Bed*
RIV3-1HC	5.8	Quartz	Illite	Kaolinite			*Blanchetown Clay*
RIV3-1HC	10.4	Quartz	Montmorillonite				*Blanchetown Clay*
RIV3-1HC	11.6	Dolomite	Quartz		Celestine		*Dolomite Bed*
RIV3-1HC	15.7	Dolomite			Quartz		*Dolomite Bed*
RIV3LC	0.8	Quartz					*Woorinen Fm*
RIV3LC	4.7	Quartz			K-feldspar		*Woorinen Fm*
RIV3LC	11.3	Quartz	Muscovite				*Loxton-Parilla Sands*
RIV4LC	1.3	Quartz	Calcite		Kaolinite		*Woorinen Fm*
RIV4LC	11.3	Quartz			Muscovite		*Loxton-Parilla Sands*
RIV4LC	17.5	Calcite	Quartz				*Murray Group Lst*
RIV5HC	5.2	Quartz	Dolomite		Smectite		*Bungunnia Lst*
RIV5HC	8.7	Quartz	Kaolinite				*Blanchetown Clay*
RIV5LC	1.7	Quartz	Dolomite	Calcite	Muscovite		*Woorinen Fm*
RIV5LC	8.3	Quartz	Calcite		Illite		*Loxton-Parilla Sands*
RIV5LC	14.3	Calcite	Quartz		Ankerite		*Murray Group Lst*
RIV6HC	6.3	Quartz	Calcite	Dolomite			*Woorinen Fm*
RIV6HC	9.7	Quartz	Kaolinite	Muscovite			*Blanchetown Clay*
RIV7HC	4.5	Quartz	Dolomite				*Woorinen Fm*
RIV7HC	34.5	Calcite	Quartz				*Murray Group Lst*
RIV7HC	39.5	Calcite	Quartz	Aragonite	Kaolinite	Illite	*Murray Group Lst*
RIV7HC	50.5	Calcite	Quartz	Aragonite	Kaolinite	Illite	*Murray Group Lst*
RIV7LC	2.5	Quartz	Muscovite	Kaolinite			*Woorinen Fm*
RIV7LC	8.5	Quartz					*Loxton-Parilla Sands*

Table 6. Continued		**Minerals**					**Interpreted**
Drill Hole	**Depth m**	**Dominant Mineral**	**Less Abundant**		**Trace**		**Unit**
RIV7LC	16.5	Quartz					*Loxton-Parilla Sands*
RIV7LC	24.5	Quartz	Calcite	Aragonite			*Murray Group Lst*
RIV7LC	40.5	Calcite	Aragonite	Quartz	Ankerite		*Murray Group Lst*
RIV7LC	47.5	Calcite	Aragonite	Quartz	Ankerite		*Murray Group Lst*
RIV7LC	57.5	Calcite	Quartz	Aragonite			*Murray Group Lst*
RIV9HC	1.5	Quartz	Calcite				*Woorinen Fm*
RIV9HC	10.5	Quartz	Kaolinite	Illite			*Blanchetown Clay*
RIV9HC	18.5	Quartz					*Loxton-Parilla Sands*
RIV9HC	22.5	Quartz					*Loxton Sands*
RIV9LC	3.5	Quartz	Dolomite				*Woorinen Fm*
RIV9LC	10.5	Quartz					*Loxton-Parilla Sands*
RIV9LC	12.5	Quartz					*Loxton-Parilla Sands*
RIV9LC	27.5	Quartz	Glauconite	Calcite	Aragonite		*Loxton Sands*